UHASSELT
KNOWLEDGE IN ACTION

Maastricht University

Faculty of Medicine and Life Sciences
School for Life Sciences
Master of Biomedical Sciences

Master's thesis

The MIF/CD74 axis in traumatic spinal cord injury: immunological characterization and role in B cell activation

Hanne Coenen

Thesis presented in fulfillment of the requirements for the degree of Master of Biomedical Sciences, specialization Molecular Mechanisms in Health and Disease

SUPERVISOR :

Prof. dr. Judith FRAUSSEN

MENTOR :

Mevrouw Serina RUBIO

2023
2024

Transnational University Limburg is a unique collaboration of two universities in two countries: the University of Hasselt and Maastricht University.

UHASSELT
KNOWLEDGE IN ACTION

www.uhasselt.be
Universiteit Hasselt
Campus Hasselt:
Martelarenlaan 42 | 3500 Hasselt
Campus Diepenbeek:
Agoralaan Gebouw D | 3590 Diepenbeek

UHASSELT
KNOWLEDGE IN ACTION

Maastricht University

Faculty of Medicine and Life Sciences
School for Life Sciences
Master of Biomedical Sciences

Master's thesis

The MIF/CD74 axis in traumatic spinal cord injury: immunological characterization and role in B cell activation

Hanne Coenen

Thesis presented in fulfillment of the requirements for the degree of Master of Biomedical Sciences, specialization Molecular Mechanisms in Health and Disease

SUPERVISOR :

Prof. dr. Judith FRAUSSEN

MENTOR :

Mevrouw Serina RUBIO

The MIF/CD74 axis in traumatic spinal cord injury: immunological characterization and role in B cell activation*

Hanne Coenen[1], Serina Rubio[1], Veerle Somers[1], and Judith Fraussen[1]

[1]Department of Immunology and Infection, Biomedical Research Institute, Hasselt University, Hasselt, Belgium

*Running title: *The MIF/CD74 Axis in B Cells in Spinal Cord Injury*

To whom correspondence should be addressed: Judith Fraussen, Tel: +32(0)11 26 92 70; Email: judith.fraussen@uhasselt.be

Keywords: Traumatic spinal cord injury, B cells, CD74, macrophage migration inhibitory factor, MIF/CD74 axis

ABSTRACT

Following traumatic spinal cord injury (SCI), B cells are activated in the periphery, migrate to the spinal cord, and contribute to an inflammatory and autoreactive immune response that leads to further damage. Recently, we demonstrated increased frequencies of CD74-expressing B cells in SCI patients. CD74 functions as a receptor for macrophage migration inhibitory factor (MIF) and in the presence of accessory proteins, including co-receptor CD44, binding of MIF to CD74 activates pathways that stimulate pro-inflammatory B cell functions. Nevertheless, the MIF/CD74 axis has not been investigated in B cells post-SCI. Here, we aimed to study the immune profile following SCI, as well as the expression and contribution of the MIF/CD74 axis to B cell activation in healthy individuals and SCI patients. Using flow cytometry, we observed higher numbers of B cells and lower NK cell numbers in acute compared to subacute and chronic phases post-injury, suggesting their involvement in earlier and later phases of SCI, respectively. Moreover, a spectral flow cytometry panel was optimized to study the expression of MIF/CD74 axis components in B cells and other immune cells. Further, using B cells of healthy individuals, we observed significant reductions in proliferation, and expression of activation markers CD80 and CD86 following CD44 blocking, as well as a pronounced decreasing trend in B cell proliferation upon MIF inhibition. Taken together, our results suggest a role for B cells and the MIF/CD74 axis in SCI, which could be further investigated as a potential target to counteract the pro-inflammatory response post-injury.

INTRODUCTION

Spinal cord injury (SCI) is defined as irreversible damage to the nerve tissue of the spinal cord, resulting in loss of sensory and motor functions (1). Each year, as many as 500,000 people suffer from SCI worldwide, of which up to 90% of the cases are of traumatic origin (2, 3). In traumatic SCI, an external physical force, such as a fall, a motor vehicle accident, or violence, initiates the injury (4-6). The prevalence of traumatic SCI is substantially higher in males (79.8%) compared to females (20.2%) (4). Moreover, the age profile of traumatic SCI patients follows a bimodal distribution with one peak in young adults (between 15 and 29 years old) and another peak in the elderly population (>50 years old) (5, 7). In the clinic, neuroprotective interventions are implemented during the acute injury phase to minimize secondary damage to the spinal cord (1). These interventions include hemodynamic management, surgical decompression, and high-dose glucocorticoid therapy (1). Nevertheless, effective treatments for SCI remain limited. Moreover, current research in the context of therapeutic development mainly focuses on the promotion of regeneration or the replacement of affected spinal cord tissue, whereas the immunopathogenesis of SCI is often disregarded (8).

The role of B cells in spinal cord injury

The sudden traumatic impact on the spine in traumatic SCI causes direct damage to the neuronal tissue, disrupts the vasculature, and compromises the blood-spinal cord barrier (9, 10). This is defined as the primary injury phase, and altogether, these events initiate a secondary injury cascade that leads to further spinal cord damage and neurological dysfunction (1, 11). This cascade is characterized by ischemia, edema, hemorrhage, the release of cytotoxic products, and immune cell infiltration (12-16). First, the innate immune system is activated, which has been demonstrated by the distribution of neutrophils, microglia, and monocytes in human post-mortem spinal cords in the first days following injury (15, 17, 18). As the time post-injury progresses from weeks to months, the adaptive immune response unfolds, as the presence of T and B cells has been observed in human SCI lesions (15, 17). The infiltration of immune cells triggers an inflammatory and autoreactive immune response that can both be protective and lead to further tissue damage in the secondary injury phase (19-25). Interestingly, previous research has indicated that B cells are activated in the periphery and contribute to this response (25-27). As demonstrated in a contusion SCI mouse model, B cells proliferate, form germinal centers (GC), and are activated in the spleen following injury (26). In addition, it was shown that the cells infiltrate and accumulate in the spinal cord, forming follicle-like structures within zones of neurodegeneration (26). Moreover, the depletion of B cells by both a genetic knockout and anti-CD20 antibodies in a mouse model of contusion and compression SCI, respectively, significantly improved locomotor activity post-injury (25, 27).

In SCI, B cells are mainly recognized for their differentiation to antibody-secreting cells, producing autoantibodies that bind central nervous system (CNS) proteins and nuclear antigens (25, 26). It has been demonstrated that these antibodies are neurotoxic since the injection of autoantibody-rich sera from SCI mice in the intact hippocampus of naive mice causes substantial astrocyte hypertrophy, microglial activation, and prominent neuron loss (26). In addition, the microinjection of antibodies purified from blood of SCI mice into the intact spinal cord of naive mice initiated full paralysis within the first 48 hours following injection (25). The autoantibodies produced following SCI caused pathology, in part, by forming antibody-antigen complexes that activate the intraspinal complement system and recruit cells bearing Fc receptors (25). Elevated titers of autoantibodies targeting CNS antigens have also been reported in the serum and plasma of SCI patients (28-30). Although less extensively studied in the context of SCI, in addition to their role in humoral immune responses, B cells exert pro-inflammatory functions that are antibody-independent, including cytokine production and the induction of T cell responses by antigen presentation and costimulation (31, 32) (Fig. 1A).

In the peripheral blood, multiple circulating B cell subsets can be identified based on the expression of subset-defining surface markers. In the bone marrow, precursor B cells develop from hematopoietic stem cells to immature B cells (33). These cells further mature from transitional ($CD24^{hi}CD38^{hi}$) B cells into naive ($IgD^{+}CD27^{-}$) B cells in the periphery (33). Subsequently, B cells can undergo a GC reaction, including proliferation, immunoglobulin isotype class switching, and affinity maturation, in which class-switched memory (CSM, $IgD^{-}CD27^{+}$) B cells can be formed (34, 35). Non class-switched memory (NCSM, $IgD^{+}CD27^{+}$) B cells are developed via a GC-independent pathway, including innate stimuli (36, 37). Lastly, double negative (DN, $IgD^{-}CD27^{-}$) B cells are thought to originate from a premature exit of the GC reaction (38). Previously, we have demonstrated decreased frequencies of naive B cells and increased frequencies of CSM B cells in chronic (cSCI, >1 month post-injury) compared to (sub)acute ((s)aSCI, ≤1 month post-injury) SCI patients (39). The latter showed similar frequencies of naive and CSM B cells as healthy controls (HC), suggesting that a shift to a memory B cell phenotype occurs during chronic SCI (39).

Based on the previously discussed findings, targeting specific B cell populations, processes, or pathways could represent a strategy to improve the recovery of SCI patients. However, the mechanisms driving pro-inflammatory B cell responses in SCI patients remain unclear.

The MIF/CD74 axis in pro-inflammatory B cell functions

Interestingly, we demonstrated significantly elevated frequencies of $CD74^{+}$ B cells in the

peripheral blood of (s)aSCI and cSCI patients compared to HC (39). Moreover, the frequency of $CD74^+$ cells was increased within all circulating B cell subsets of (s)aSCI and cSCI patients (39). CD74 intracellularly functions as a major histocompatibility complex class II chaperone and is therefore mostly expressed in antigen-presenting cells (40). In addition to its role in antigen presentation, CD74 that is expressed on the cell surface has a function in immune cell stimulation by serving as a receptor for the pro-inflammatory cytokine macrophage migration inhibitory factor (MIF) (41). MIF is produced by a variety of cell types, including immune, endocrine, endothelial, and epithelial cells (42). Among blood immune subsets of healthy individuals, MIF has been described to be predominantly expressed by B cells compared to T cells, dendritic cells, and monocytes (43).

In B cells, the binding of MIF to CD74 leads to the initiation of various downstream signaling pathways that activate the cells to exert pro-inflammatory functions, such as proliferation, survival, migration, and cytokine production (43-48). However, it has been demonstrated that the recruitment of accessory proteins, including the co-receptor CD44 and CXC-motif chemokine receptors (CXCRs), is needed to elicit MIF signaling through CD74 and activate these inflammatory functions (49-51). Besides MIF binding to CD74, the recruitment of CD44 was necessary to initiate a signaling cascade in murine splenic B cells, inducing the phosphorylation of spleen tyrosine kinase (Syk), which activated the serine/threonine kinase Akt in a phosphatidylinositol 3'-kinase (PI3K)-dependent manner (44, 48). This stimulated the intramembrane cleavage of CD74 and the phosphorylation and activation of nuclear factor κB (NF-κB), resulting in upregulated expression of survival factors B-cell lymphoma (Bcl)-2 and Bcl-extra-large (xL). In addition, the expression of cyclin E, which is expressed upon initiation of the S-phase of the cell cycle, was upregulated following the binding of MIF to the CD74/CD44 complex. These pathways stimulated the survival and proliferation of murine splenic B cells (44, 48). Furthermore, triggering of the cognate receptor of MIF, CD74, induced the expression of pro-inflammatory cytokines interleukin (IL)-6 and tumor necrosis factor (TNF)-α via NF-κB in human B cells (43). However, the specific co-receptors involved and underlying pathway remain unknown. In contrast, the simultaneous binding of MIF to both CD74 and CXCR4 or -7 was necessary to initiate the phosphorylation of zeta-chain-associated protein kinase (ZAP)-70 and extracellular signal-regulated kinase (ERK), which was essential to facilitate migration of murine splenic B cells in response to MIF (45, 46). In addition to CXCR4 and -7, CXCR2 has been demonstrated to form receptor complexes with CD74 and trigger chemotaxis of monocytes (50). Nevertheless, CXCR2 expression was low on murine splenic B cells and is, therefore, unlikely to be involved in B cell migration (45, 46). Furthermore, MIF stimulation of B cells resulted in intracellular calcium mobilization and F-actin polymerization, which both have been associated with cell migration (46) (Fig. 1B).

The MIF/CD74 axis has been demonstrated to be dysregulated in B cells in various immune system-related diseases. Over-expression of CD74, CD44, and MIF in spleen-derived B cells was shown in a mouse model of systemic lupus erythematosus (52). Nevertheless, in multiple sclerosis (MS) patients, downregulation of CD74 and MIF in circulating B cells was demonstrated (43). In contrast, the expression of chemokine receptor CXCR4 on B cells was upregulated in these patients. Moreover, CD74 boosted the pro-inflammatory and proliferative capacity of B cells, whereas CXCR4 prevented apoptosis of these cells. In addition, CD74 and CXCR4 were differentially expressed in transitional and naive mature compared to CSM and NCSM B cells, suggesting that the MIF/CD74 axis may play a role in the differentiation and activation of these B cell subsets in MS (43). Lastly, B cells of chronic lymphocytic leukemia patients strongly over- and co-expressed CD74 and CXCR4 (53). Furthermore, the MIF-induced activation and interaction between both receptors stimulated survival and migration of malignant B cells (53).

The MIF/CD74 axis in spinal cord injury

Multiple studies have indicated the role of MIF in SCI pathology. Following contusion- and compression-induced SCI in rats, upregulation of MIF expression in the spinal cord has been demonstrated (54-57). Furthermore, MIF deletion reduced neuronal death and promoted functional

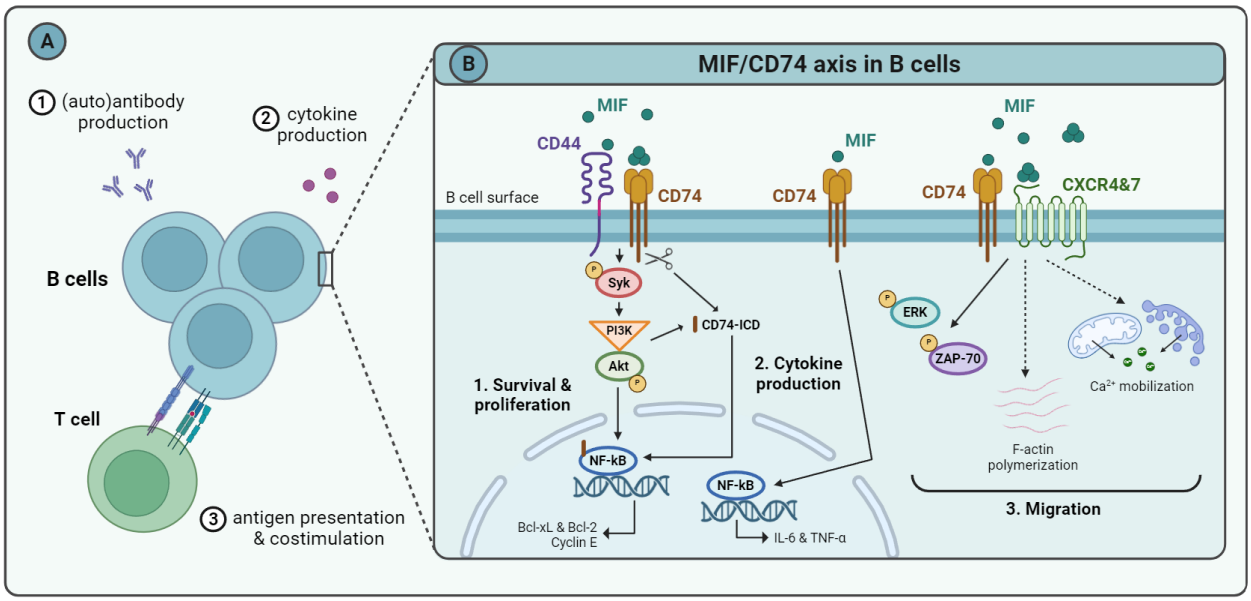

Figure 1: B cell effector functions and the role of the MIF/CD74 signaling pathway. A) B cells exert different effector functions, including the differentiation to antibody-secreting cells, producing (auto)antibodies (1), cytokine production (2), and antigen presentation and costimulation in the induction of T cell responses (3). **B**) MIF promotes B cell survival and proliferation following binding to a complex of CD74 and CD44 (1), cytokine production by B cells after binding CD74 (2), and B cell migration by binding to a complex of CD74 and CXCR2, -4, or -7 (3). For functions indicated with a dashed line, the direct link between receptor binding and the effect remains unconfirmed. *Akt, protein kinase B; Bcl-xL, B-cell lymphoma-extra-large; Bcl-2, B-cell lymphoma-2; CXCR, CXC-motif chemokine receptor; Ca^{2+}, calcium; ERK, extracellular signal-regulated kinase; ICD, intracellular domain; IL, interleukin; MIF, macrophage migration inhibitory factor; NF-κB, nuclear factor κB; PI3K, phosphatidylinositol 3-kinase; Syk, spleen tyrosine kinase; TNF, tumor necrosis factor; ZAP-10, zeta-chain-associated protein kinase-70.* Created using BioRender.

recovery following compression-induced SCI in mice, suggesting that the presence of MIF hinders neuronal survival after SCI (58). Interestingly, it was shown that MIF promotes neuronal death through the induction of oxidative stress and the activation of apoptotic pathways (59). Moreover, MIF has been demonstrated to enhance the recruitment of inflammatory cells to the injured site of the spinal cord and to stimulate the production of pro-inflammatory cytokines by astrocytes, microglia, and leukocytes following SCI (54, 55, 57, 60). In addition to elevated CD74 expression on B cells, we have shown that SCI patients showed a trend toward increased MIF levels in plasma (39). This has been confirmed by other research groups reporting elevated plasma levels of MIF in acute and chronic SCI patients (61-63).

Although previous studies have investigated the role of the MIF/CD74 axis in pro-inflammatory B cell functions and in SCI, individually, the axis has not been studied in B cells following SCI. Therefore, further research addressing the involvement of the MIF/CD74 signaling pathway in post-SCI B cell responses is needed. Here, we aimed to study the expression and contribution of the MIF/CD74 axis to the pro-inflammatory characteristics of B cells in healthy individuals and SCI patients. First, the absolute number of B cells and other major immune cell subsets, including T cells, natural killer (NK) cells, dendritic cells (DC), and monocytes, was monitored following traumatic SCI. Second, a spectral flow cytometry panel was optimized to study the surface expression of the receptors of the MIF/CD74 axis and the intracellular expression of MIF in B cells and other immune cell subsets. Lastly, *in vitro* proliferation and activation of B cells were investigated upon selective inhibition of the MIF/CD74 axis. In the search for targeted therapies for SCI, this study might contribute to the identification of novel immune- and B cell-related targets to intervene in the secondary injury phase of SCI.

EXPERIMENTAL PROCEDURES

Study subjects – Traumatic SCI patients without autoimmune disorders were recruited at Hospital Oost-Limburg (Genk, Belgium), University Hospital Leuven (Leuven, Belgium), Jessa Hospital (Hasselt, Belgium), and Adelante Centre of Expertise in Rehabilitation (Hoensbroek, The Netherlands). Patients were examined according to the American Spinal Injury Association (ASIA) impairment scale (AIS) (64). HC were recruited at Hasselt University (Hasselt, Belgium). Ethical approval was acquired from Medical Ethics Committee Hasselt University, Medical Ethics Committee Hospital Oost-Limburg, and Medical Ethics Review Committee Maastricht UMC+. Written informed consent was obtained from all participants conforming to the Declaration of Helsinki. Samples were cryopreserved at the University Biobank Limburg. In total, 42 SCI samples were included at different time points: <1 week (n=5), 3 weeks (n=5), 4 weeks (n=3), 7 weeks (n=5), 12 weeks (n=6), 18 weeks (n=5), 6 months (n=8), and 1 year (n=5) post-injury. The acute, subacute, and chronic phases were defined as ≤4 weeks, 7-18 weeks, and ≥6 months post-injury, respectively. Clinical data of the study subjects are provided in Table 1 and Table S1.

Cell isolation – Peripheral blood mononuclear cells (PBMC) were isolated from whole blood by Ficoll density gradient centrifugation (Lympholyte: Cedarlane Laboratories, SanBio B.V., Uden, The Netherlands). PBMC were cryopreserved in 20% DMSO (AppliChem, Darmstadt, Germany) in fetal bovine serum (FBS) (Gibco, Schwerte, Germany) and stored in liquid nitrogen until used. After thawing, PBMC were centrifugated for 10 min at 300xg at 4°C and recovered in 20% FBS/RPMI 1640 (Lonza, Verviers, Belgium) and 0.5 mg/ml DNAse (Sigma-Aldrich, Hoeilaart, Belgium) for 10 min at 37°C. After two washing steps in 20% FBS/RPMI 1640, the cells were resuspended in culture medium (CM; RPMI 1640, 10% FBS, 1% nonessential amino acids, 1% sodium pyruvate, 50 U/ml penicillin and 50 mg/ml streptomycin (all Sigma-Aldrich)). PBMC were counted using a Moxi cell counter (Orflo, Ketchum, U.S.). For *in vitro* assays, B cells were isolated using the EasySep™ Human B Cell Enrichment Kit (STEMCELL Technologies SARL, Saint-Egrève, France; #19054), following the manufacturer's instructions. Purity of the isolated B cells was confirmed on an LSRFortessa flow cytometer (BD Biosciences, Erembodegem, Belgium) following CD19 staining and was routinely > 99.0%.

Table 1 – Characteristics of study subjects.

Cell counts	SCI	HC
n	16	2
Biological sex (n males, %)	13 (81.3)	0 (0)
Age (years, SD)	55.3 (18)	45.5 (7.8)
Level of injury (n, %)		
Cervical	12 (75)	/
Thoracic	4 (25)	/
AIS score		
A	3 (18.75)	/
B	1 (6.25)	/
C	2 (12.5)	/
D	6 (37.5)	/
Not available	4 (25)	/
Included time points (n, %)		
<1 week	5 (31.25)	/
3 weeks	5 (31.25)	/
4 weeks	3 (18.75)	/
7 weeks	5 (31.25)	/
12 weeks	6 (37.5)	/
18 weeks	5 (31.25)	/
6 months	8 (50)	/
1 year	5 (31.25)	/
MIF/CD74 axis screening		
n	/	2
Biological sex (n males, %)	/	1 (50)
Age (years, SD)	/	36.5
Activation and proliferation assay		
n	/	11
Biological sex (n males, %)	/	1 (9)
Age (years, SD)	/	39.0 (11.4)

AIS, American Spinal Injury Association impairment scale; HC, healthy control; MIF, macrophage migration inhibitory factor; SCI, spinal cord injury; SD, standard deviation.

Cell counts – The absolute number of B cells, T cells, NK cells, DC, and monocytes was determined using whole blood. Fc receptors were blocked using human FcR Blocking Reagent (1/20; BioLegend, London, U.K.; #422302) for 10 min at room temperature (RT). Subsequently, the blood was incubated with anti-human monoclonal antibodies against CD3, CD14, CD19, CD45, CD56, and HLA-DR (Table S2) for 15 min at RT. This was followed by incubation with RBC Lysis/Fixation (1x) solution (BioLegend; #422401) for 15 min at RT and administration of Precision Count Beads (BioLegend; #424902), following the manufacturer's instructions. Blood samples were acquired on an LSRFortessa flow cytometer, and absolute cell numbers were calculated following the manufacturer's instructions (using Formula S1).

MIF/CD74 axis screening – A flow cytometry panel consisting of 25 immune cell markers was optimized (Table S3). Staining was carried out on $1x10^6$ PBMC seeded in 96-well V-bottom plates. Flow cytometry for all steps was performed on the Cytek® Aurora spectral flow cytometer (Cytek Biosciences, Fremont, California).

Surface antibody titrations: PBMC were single-stained with anti-human monoclonal or recombinant surface antibodies included in the panel (Table S3). Besides the recommended dilution, at least three other dilutions were tested. If needed, subset-specific markers were stained in combination with subset-defining markers.

Intracellular MIF titration: $1x10^6$ PBMC were seeded in 24-well culture plates and treated with phorbol 12-myristate 13-acetate (PMA; 50 ng/ml; #P1585), Calcium Ionophore A23187 (1 µg/ml; #C9275) (both Sigma-Aldrich), and GolgiStop (4 µl/6 ml, BD Biosciences; #554715) in CM for 4h at 37°C. Subsequently, cells were transferred to 96-well V-bottom plates and stained using an anti-CD19 antibody (Table S3) in flow cytometry buffer (5% FB; 1xPBS (Gibco), 5% FBS, 0.1% sodium azide (NaN_3; Sigma-Aldrich)) for 15 min at 37°C. Next, cells were fixed and permeabilized with the Fixation/Permeabilization Solution Kit (BD Biosciences; #554715), following the manufacturer's instructions. Lastly, cells were transferred to 96-well U-bottom plates and stained with an anti-MIF antibody (1/80 and 1/200) for 30 min or overnight at 4°C (Table S3).

Co-staining versus consecutive staining of viability dye and IgG: PBMC were simultaneously stained with Zombie NIR™ dye and an anti-IgG antibody (Table S3) in 1xPBS or 1xPBS/2%FBS (2% FB) for 15 min at RT. Alternatively, cells were stained using the Zombie NIR™ dye in 1xPBS, followed by an antibody staining against IgG in 5% FB, both for 15 min at RT.

Single stains at RT versus 37°C: PBMC were stained using antibodies against CD3, CD4, CD8, CD11c, CD14, CD16, CD21, CD24, CD38, CD45RA, CD56, CXCR2, HLA-DR, IgA, and IgM (Table S3) in 5% FB for 15 min at RT or in 5% NaN_3-free FB for 30 min at 37°C.

Co-staining of viability dye, IgG, and other markers – PBMC were stained with Zombie NIR™ and an anti-IgG antibody in 1xPBS for 15 min at RT followed by staining using antibodies against CD11c, CD14, CD16, CD24, and CD45RA in 5% FB for 15 min at RT. Alternatively, cells were co-stained with Zombie NIR™ and antibodies against IgG, CD11c, CD14, CD16, CD24, and CD45RA in 1xPBS for 15 min at RT.

Activation and proliferation assay – Following isolation, primary B cells were labeled with carboxyfluorescein succinimidyl ester (CFSE; 0.5 µM, BioLegend) for 20 min at 37°C and seeded in 96-well U-bottom plates at $1x10^5$ cells in CM. B cells were stimulated with goat $F(ab')_2$ anti-human IgG/IgA/IgM (1 µg/ml; Jackson ImmunoResearch Europe, Suffolk, U.K.; #109-006-064) and CpG oligonucleotides (ODN 2006, 1 µg/ml; Invivogen, Toulouse, France; #tlrl-2006) for 72h at 37°C. After 24h, complete stimulation was achieved by adding CD40 ligand (CD40L, 1 µg/ml; BioLegend; #591704). Following stimulation, different concentrations of blocking antibodies against CD74 (Southern Biotech, Birmingham, USA; #9775-14) and CD44 (ThermoFisher, Geel, Belgium; #MA4400), and a small molecule inhibitor of MIF (R&D Systems, Minneapolis; USA; #4288/10), together with their respective controls, were used to individually block or antagonize their function for 24, 48, or 72h (Table S4). After 72h, B cells were transferred to 96-well V-bottom plates and stained with Fixable Viability Dye eFluor 780 (1/1000; eBioscience, San Diego, USA) in 1xPBS for 30 min at 4°C, and anti-human monoclonal antibodies against CD19, CD80, and CD86 or CD25 (Table S5) in 5% FB for 15 min at RT. Flow cytometry was performed on an LSRFortessa flow cytometer.

Data and statistical analysis – Flow cytometry data was analyzed using FlowJo v10.10.0 (BD Life Sciences, Oregon, USA). Statistical analysis was performed using JMP Pro 17.0 (SAS Institute, Cary, NC, USA) and GraphPad Prism version 10.2.3 (GraphPad Software, San Diego, CA, USA). Differences in immune cell counts between time points and phases post-SCI were analyzed using linear mixed models. As a first exploratory analysis, age at primary injury was included as a covariate. To consider association of measurements within the same patient, patient ID was included as a random effect. Correlations between cell counts and days post-injury were performed using Spearman correlation tests. For *in vitro* blocking assays, normal distribution was verified with the Shapiro-Wilk test. A paired t-test was performed to analyze normally distributed data. Otherwise, a

Wilcoxon Signed-Rank test was performed. A p-value of <0.05 was considered significant.

RESULTS

Absolute B cell numbers were increased, whereas NK cell numbers were reduced in the acute versus the subacute and chronic phases post-SCI – First, the absolute count of major immune cell subsets was analyzed in whole blood of HC and SCI patients. These included B cells, T cells, NK cells, DC, and monocytes. An overview of the used gating strategy is shown in Fig. S1. For SCI patients, cell counts were monitored at eight time points following injury, from <1 week up to 1 year post-injury. Comparison of cell counts at the different time points post-injury showed no significant differences for the different subsets (Fig. 2). However, when cell counts at <1 week post-injury were compared to HC values, respectively, absolute numbers of B cells (102.8 ± 62.15 vs. 11.90 ± 4.508 cells/µl), T cells (502.4 ± 204.3 vs. 194.5 ± 14.62 cells/µl), DC (5.150 ± 7.715 vs. 2.052 ± 0.2489 cells/µl) and monocytes (221.8 ± 157.4 vs. 78.92 ± 12.62 cells/µl) all showed an increased trend (Fig. 2). Although acute absolute NK cell counts were not increased in comparison to HC (133.6 ± 52.24 vs. 201.9 ± 7.441 cells/µl; Fig. 2C), a positive correlation was observed for these cells with time post-injury (r = 0.3315, p = 0.0320; Fig. S2). No correlations were observed for the other immune cell subsets (Fig. S2).

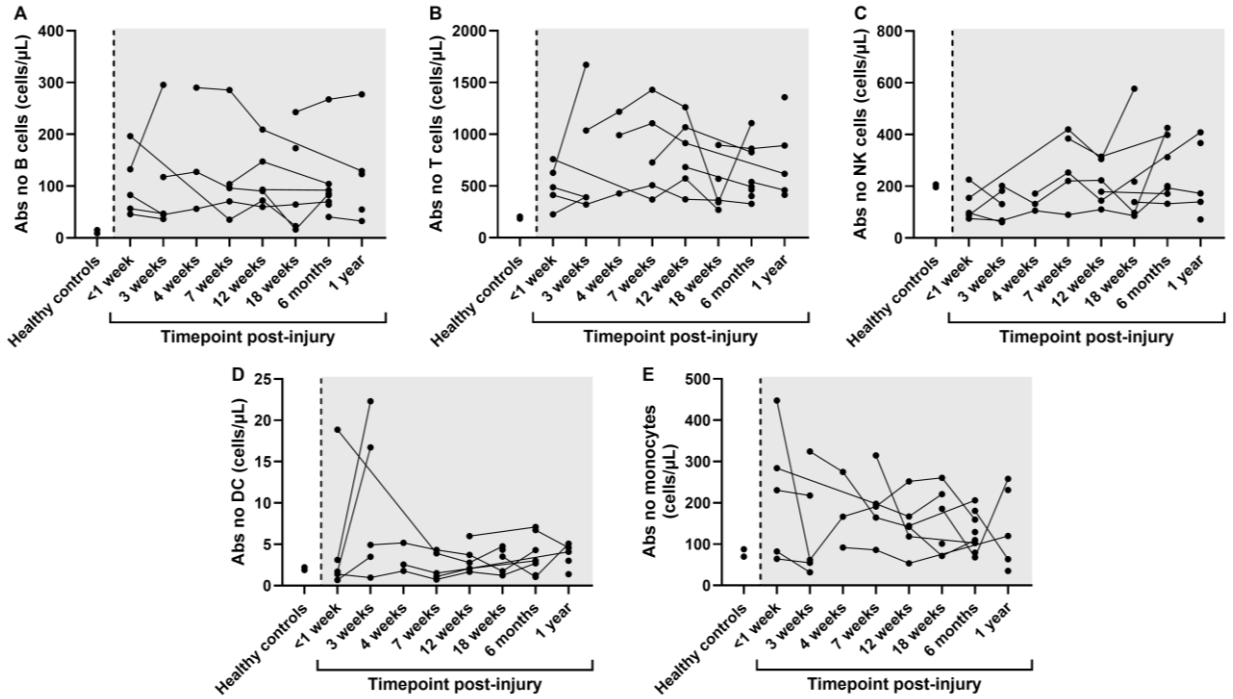

Figure 2 – Absolute number of major immune cell subsets in whole blood of HC and SCI patients at different time points post-injury. The absolute numbers (cells/µl) of B cells (**A**), T cells (**B**), NK cells (**C**), DC (**D**), and monocytes (**E**) in whole blood were calculated using count beads for healthy controls (n=2) and SCI patients (n=16) at different time points post-injury. Data of SCI patients were subdivided into eight time categories: <1 week (n=5), 3 weeks (n=5), 4 weeks (n=3), 7 weeks (n=5), 12 weeks (n=6), 18 weeks (n=5), 6 months (n=8), and 1 year (n=5). Each dot represents data from a single blood sample and samples belonging to the same SCI patient are connected with a line. Time points post-injury were statistically compared using a linear mixed model with age as a covariate. *Abs no; absolute number; DC, dendritic cells; NK, natural killer.*

In addition, the absolute cell counts were compared between acute (≤4 weeks post-SCI), subacute (7-18 weeks post-SCI), and chronic (≥6 months post-SCI) phases post-injury. B cells were significantly increased in the acute in comparison to the subacute phase (117.6 ± 90.72 vs. 111.4 ± 79.26 cells/µl; p = 0.0157), as well as the acute versus the chronic phase of SCI (117.6 ± 90.72 vs.

109.5 ± 77.76 cells/µl; p = 0.0266; Fig. 3A). Moreover, absolute numbers of NK cells were significantly higher at chronic stages compared to acute stages (245.5 ± 120.3 vs. 130.3 ± 53.64 cells/µl; p = 0.0009), and at subacute versus acute stages (235.0 ± 137.6 vs. 130.3 ± 53.64 cells/µl; p = 0.0156; Fig. 3C). No significant changes were demonstrated for T cells, DC, and monocytes (Fig. 3B, D, and E)

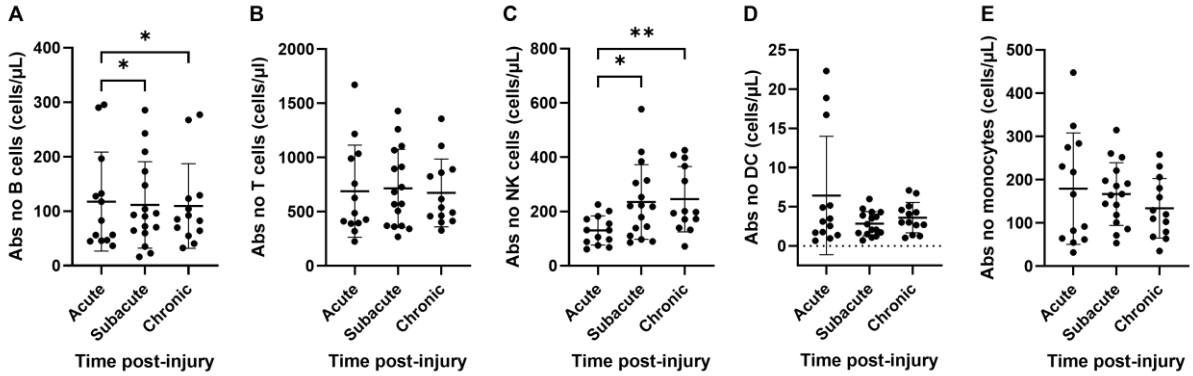

Figure 3 – Absolute number of major immune cell subsets in whole blood of SCI patients at acute, subacute, and chronic phases post-injury. The absolute numbers (cells/µl) of B cells (**A**), T cells (**B**), NK cells (**C**), DC (**D**), and monocytes (**E**) in whole blood of SCI patients (n=16) were calculated using count beads at acute (n=7, including 13 samples), subacute (n=8, including 16 samples), and chronic (n=11, including 13 samples) phases post-injury. Each dot represents data from a single blood sample. Mean (bars) ± SD is depicted for each group. Study groups were statistically compared using a linear mixed model with age as a covariate. *p < 0.05; **p < 0.01. *Abs no; absolute number; DC, dendritic cells; NK, natural killer.*

Optimization of a spectral flow cytometry panel for MIF/CD74 axis screening in HC versus SCI patients – To study the expression of the MIF/CD74 axis in major immune cell and B cell subsets in peripheral blood of SCI patients and HC, a spectral flow cytometry panel was optimized. Following panel design, antibodies to classify immune cells, and to study the axis receptors and intracellular MIF were titrated individually (Table S3).

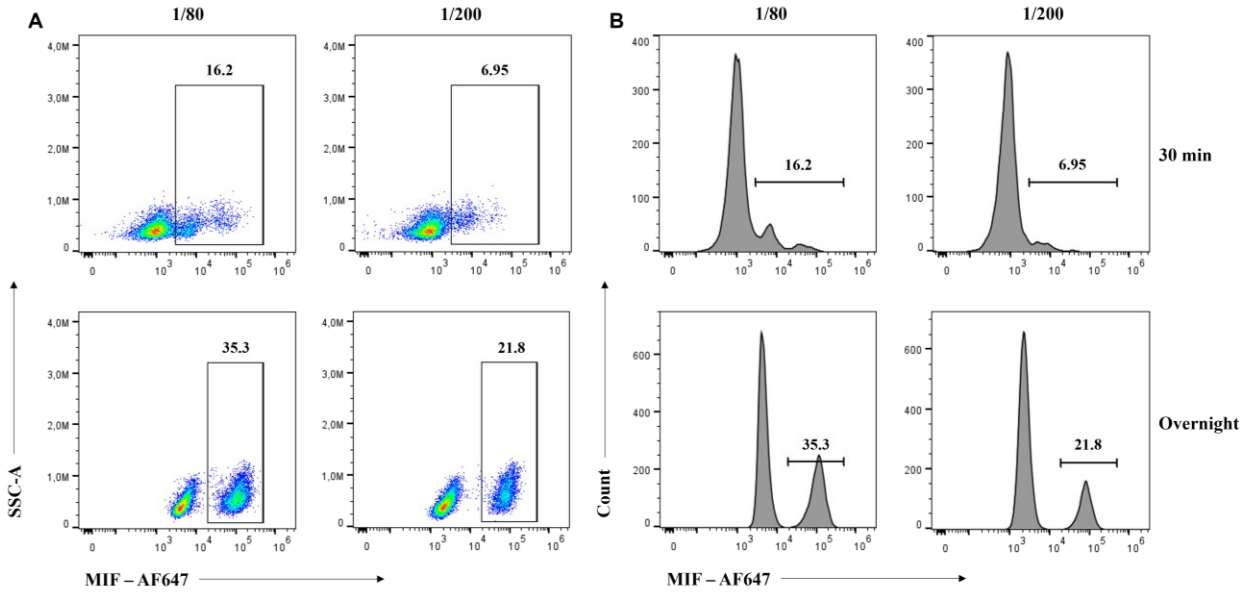

Figure 4 – MIF intracellular staining titration. Total PBMC of HC (n=1) were treated with PMA, calcium ionophore, and GolgiStop. Subsequently, the cells were stained with antibodies targeting surface CD19 (1/250) and

intracellular MIF, respectively. Two dilutions of anti-MIF antibody (1/80 and 1/200) and both 30-minute and overnight staining were tested. Data are shown as scatter plots (**A**) and histograms (**B**) and were gated on single human CD19$^+$ B cells. Frequencies of the positive population are depicted. *AF, Alexa Fluor; HC, healthy control; MIF, macrophage migration inhibitory factor; min, minutes; PMA, phorbol 12-myristate 13-acetate; SSC-A, side scatter area.*

Intracellular MIF staining within CD19$^+$ B cells was tested in two dilutions (1/80 and 1/200) and incubated for either 30 minutes or overnight. The best resolution between MIF-negative and -positive populations was shown upon overnight staining using a dilution of 1/80 (Fig. 4A-B).

To screen for the MIF/CD74 axis, cells will be treated with Fc receptor blocking solution, which contains specialized human IgG. To avoid aspecific binding, cells need to be stained for surface IgG prior to Fc receptor blocking. Ideally, this staining will be combined with the viability staining. Therefore, co-staining in either 2% FB (Fig. 5A) or 1xPBS (Fig. 5B), as well as consecutive staining with the viability dye and an antibody targeting surface IgG (Fig. 5C), were compared. As expected, the resolution between dead and viable cells was highest upon consecutive staining of the markers (Fig. 5A). Nevertheless, dead and viable cells could still be well distinguished when simultaneous staining was performed in 1xPBS (Fig. 5B), whereas this was no longer the case when stained in 2% FB (Fig. 5C). A similar resolution between and frequency of IgG-negative and -positive populations were observed for all staining conditions (Fig. 5A-C).

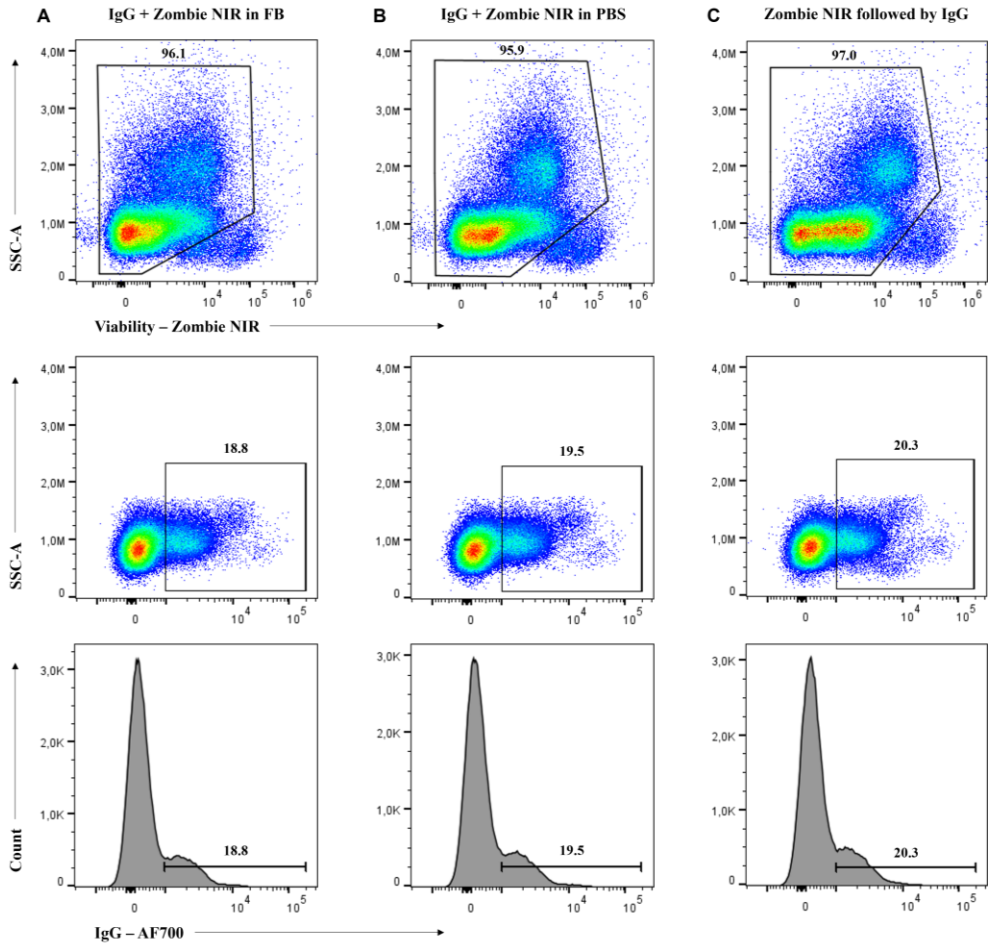

Figure 5 – Co-staining versus consecutive staining of Zombie NIR and IgG. Total PBMC of HC (n=1) were stained with Zombie NIR viability dye (1/4000) and an antibody targeting surface IgG (1/20). Staining was performed simultaneously in 2% FB (**A**) or 1xPBS (**B**), or respectively (**C**). Data are shown as scatter plots for

Zombie NIR, gated on total single lymphocytes, and as scatter plots and histograms for IgG, gated on single viable lymphocytes. Frequencies of living and IgG^+ cells are depicted. *AF, Alexa Fluor; 2% FB, flow cytometry buffer (1xPBS/2% FBS); FBS, fetal bovine serum; HC, healthy control; IgG, immunoglobulin G; 1xPBS, phosphate buffered saline; SSC-A, side scatter area.*

Staining at 37°C and avoiding the use of NaN_3 in the staining solution can improve the detection of chemokine receptors, as shown here for CXCR2 (Fig. 6A). Therefore, other surface markers of the panel were stained at 37°C in 5% NaN_3-free FB versus at RT in 5% NaN_3-containing FB. Higher resolution between negative and positive populations was observed at RT for CD45RA (Fig. 6B), as well as for CD11c, CD14, CD16, and CD24 (data not shown). In contrast, CD56 (Fig. 6C), CD3, CD4, CD8, CD21, CD24, HLA-DR, IgA, and IgM (data not shown), showed similar resolutions at both staining conditions and could therefore be stained simultaneously with the CXCR at 37°C in NaN_3-free FB.

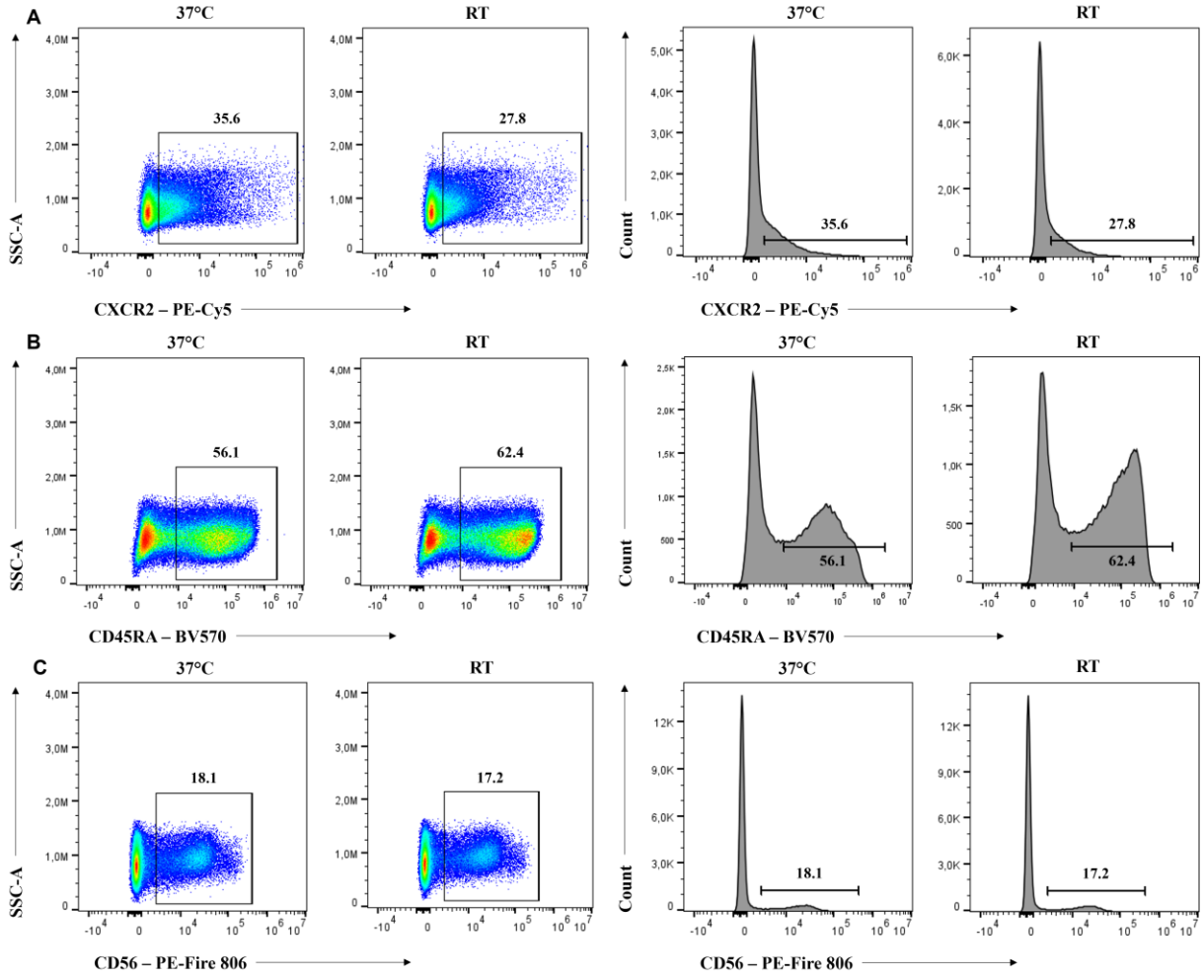

Figure 6 – Single stains of CXCR2, CD45RA, and CD56 at RT versus 37°C. Total PBMC of HC (n=1) were stained with antibodies targeting CXCR2 (1/20; **A**), CD45RA (1/100; **B**), CD56 (1/200; **C**) at 37°C in 5% FB without NaN_3 and at RT in 5% FB with NaN_3. Data are shown as scatter plots and histograms and were gated on single total lymphocytes. Frequencies of the positive population are depicted. *BV, Brilliant Violet; CD, cluster of differentiation; 5% FB, flow cytometry buffer (1xPBS/5% FBS); FBS, fetal bovine serum; HC, healthy control; NaN_3, sodium azide; PBS, phosphate buffered saline; PE-Cy, Phycoerythrin-Cyanine; PE-Fire, Phycoerythrin-Fire; RT, room temperature; SSC-A, side scatter area.*

To minimize staining steps in the final MIF/CD74 axis screening protocol, staining of the markers preferably stained at RT, which are CD11c, CD14, CD16, CD24, and CD45RA, was tested simultaneously with the Zombie NIR and IgG staining in 1xPBS (Fig. 7A-E).

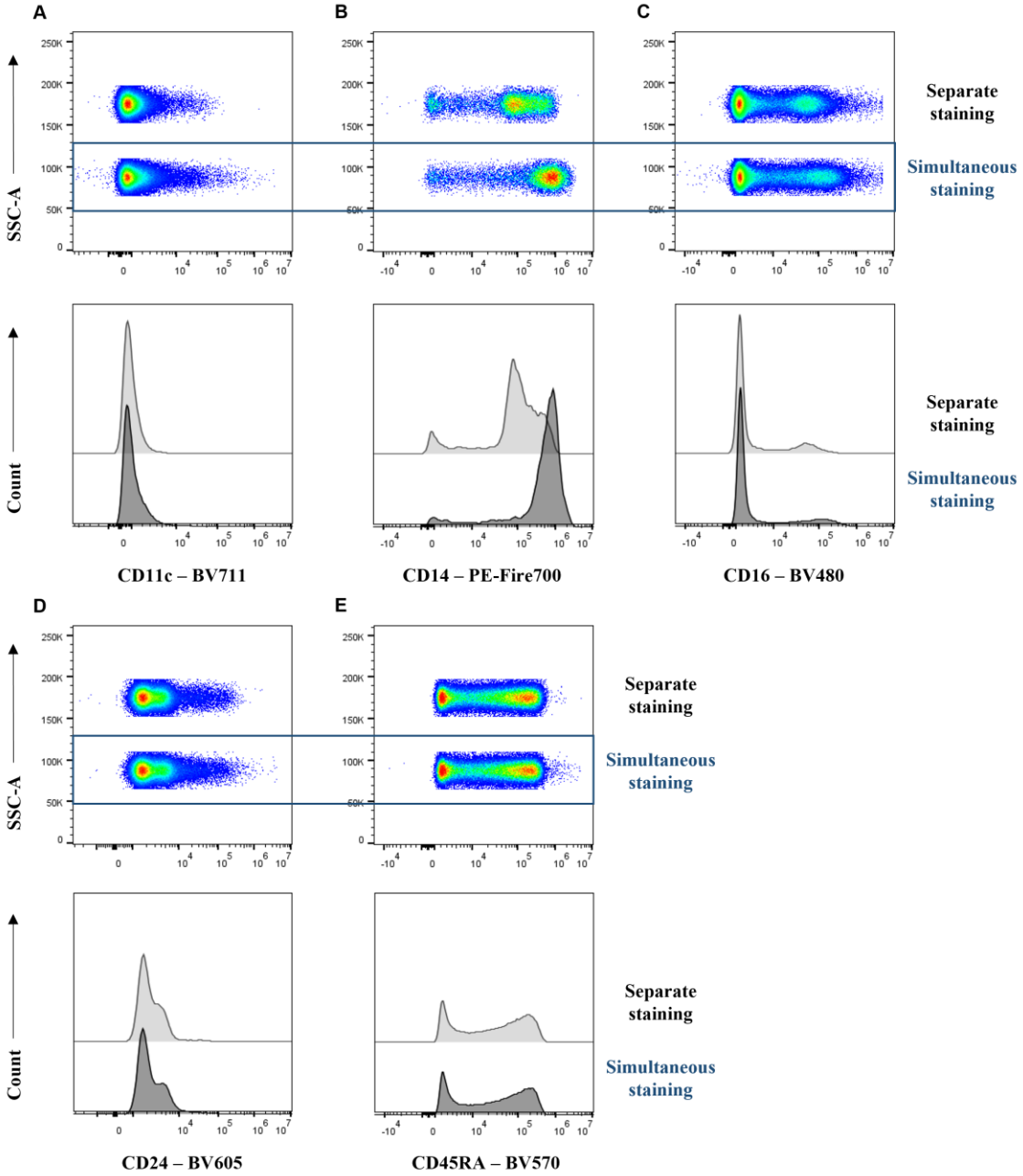

Figure 7 – Co-staining of Zombie NIR, IgG, CD11c, CD14, CD16, CD24, and CD45RA at RT. Total PBMC of HC (n=1) were stained with Zombie NIR viability dye (1/4000) and anti-IgG antibody (1/20) in 1xPBS, followed by staining of CD11c (1/50; **A**), CD14 (1/2000; **B**), CD16 (1/200; **C**), CD24 (1/20; **D**), and CD45RA (1/100; **E**) in 5% FB at RT (separate staining; upper plots and histograms). Alternatively, simultaneous staining with Zombie NIR and antibodies targeting IgG, CD11c, CD14, CD16, CD24, and CD45RA in 1xPBS was performed at RT (simultaneous staining; lower plots and histograms). Data are shown as concatenated scatter plots and overlay histograms. *BV, Brilliant Violet; CD, cluster of differentiation; 5% FB, flow cytometry buffer (1xPBS/5% FBS); FBS, fetal bovine serum; HC, healthy control; PE, Phycoerythrin; RT, room temperature; SSC-A, side scatter area.*

For comparison, a separate staining of Zombie NIR and anti-IgG antibody in 1xPBS followed by the other markers in 5% FB was performed (Fig. 7A-E). Upon comparison of both staining conditions, similar to higher resolutions between negative and positive populations were observed for all the included markers (Fig. 7A-E).

Blocking CD44 and MIF signaling reduces primary B cell proliferation – To determine how the cognate receptor of MIF, CD74, its co-receptor CD44, and MIF itself influence the function of B cells, the proliferation and activation potential of *in vitro*-stimulated B cells of HC was studied upon blocking with different concentrations and incubation times of blocking antibodies against CD74 and CD44, and a small molecule inhibitor for MIF. An overview of the used gating strategy is shown in Fig. S3.

Treatment of primary B cells with a CD74 blocking antibody at concentrations of 10, 20, and 40 µg/ml for 48 and 72 hours had minor effects on proliferation compared to its isotype control (at 48h, 10 µg/ml: 0.9827; 20 µg/ml: 0.9512; 40 µg/ml: 0.9380; at 72h, 10 µg/ml: 0.9455; 20 µg/ml: 0.9913 ± 0.06633; 40 µg/ml: 0.9228 ± 0.01750; Fig. 8A-B). Upon blocking with an anti-CD44 antibody, primary B cell proliferation was not affected at 24 hours incubation time (10 µg/ml: 0.9969; 20 µg/ml: 1.008; 40 µg/ml: 0.9845; Fig. 8D). However, more pronounced effects were seen at a longer incubation time of 48 hours, reaching significance at concentrations of 10 and 40 µg/ml (1 µg/ml: 0.9489; 10 µg/ml: 0.8305 ± 0.05239, p = 0.0006; 20 µg/ml: 0.8648 ± 0.2290; 40 µg/ml: 0.8238 ± 0.2236, p = 0.0095). Similarly, reductions in primary B cell proliferation were observed upon incubation for 72 hours, which were also significant at concentrations of 10 and 40 µg/ml (1 µg/ml: 0.9260; 10 µg/ml: 0.8083 ± 0.07623, p = 0.0033; 20 µg/ml: 0.7459; 40 µg/ml: 0.8070 ± 0.04805, p = 0.0095; 100 µg/ml: 0.8530; Fig. 8C-D). Even more pronounced reductions in primary B cell proliferation were observed upon treatment with MIF inhibitor (ISO1), with trends toward concentration- and duration-dependent effects. At concentrations 10 and 100 µM, no or only slight changes in B cell proliferation were demonstrated at incubations times of 24 hours (10 µM: 1.015; 100 µM: 0.9631 ± 0.04325), 48 hours (10 µM: 0.9742; 100 µM: 1.046 ± 0.08307), and 72 hours (10 µM: 0.9501; 100 µM: 0.9095 ± 0.04534; Fig. 8F). However, larger reductions were shown at concentrations of 500 and 1000 µM, increasing with concentration and incubation time (at 24h, 500 µM: 0.7583; 1000 µM: 0.3123 ± 0.08709; at 48h, 500 µM: 0.5000; 1000 µM: 0.2718 ± 0.1509; at 72h, 500 µM: 0.3173; 1000 µM: 0.1602 ± 0.1283; Fig. 8E-F).

Second, activation marker expression (CD80, CD86, and CD25) by primary B cells was studied upon blocking of the CD74 receptor, CD44 receptor and MIF. Blocking with anti-CD74 antibody minimally affected both CD80 (at 48h, 10 µg/ml: 0.8984; 20 µg/ml: 0.9817; 40 µg/ml: 0.9847; at 72 hours, 10 µg/ml: 1.044; 20 µg/ml: 1.002 ± 0.05947; 40 µg/ml: 0.9989 ± 0.03416; Fig. 9A) and CD86 expression (at 48h, 10 µg/ml: 1.004; 20 µg/ml: 0.9662; 40 µg/ml: 1.005; at 72h, 10 µg/ml: 1.202; 20 µg/ml: 1.012 ± 0.008704; 40 µg/ml: 1.001 ± 0.02512; Fig. 9B) upon all tested concentrations and incubation times. Similarly, minor changes in CD80 expression were observed upon CD44 blocking compared to treatment with isotype control (at 24h, 10 µg/ml: 0.9197; 20 µg/ml: 0.9789; 40 µg/ml: 0.9601; at 48h, 1 µg/ml: 0.9432; 20 µg/ml: 0.9784 ± 0.07142; 40 µg/ml: 0.9001 ± 0.08930, p = 0.2007; at 72h, 1 µg/ml: 0.9487; 10 µg/ml: 0.9346 ± 0.06329, p = 0.0847; 20 µg/ml: 0.9940; 40 µg/ml: 0.9490 ± 0.07865, p = 0.3401; 100 µg/ml: 0.9308; Fig. 9C). Nevertheless, statistical significance was reached at a concentration of 10 µg/mL with an incubation time of 48 hours (0.9098 ± 0.03835, p = 0.0170; Fig. 9C). More pronounced reductions were shown for CD86 expression (at 24h, 10 µg/ml: 0.8434; 20 µg/ml: 0.8622; 40 µg/ml: 0.8912; at 48h, 1 µg/ml: 0.8446; 20 µg/ml: 0.9445 ± 0.1716; 40 µg/ml: 0.8086 ± 0.08659, p = 0.0787; at 72h, 1 µg/ml: 0.8120; 20 µg/ml: 0.8883; 40 µg/ml: 0.8613 ± 0.06619, p = 0.0897; 100 µg/ml: 0.9529) and significant differences compared to the isotype control were demonstrated at the concentration of 10 µg/ml at incubation periods of 48 (0.8528 ± 0.04228, p = 0.0029) and 72 hours (0.8581 ± 0.03596, p = 0.0019; Fig. 9D).

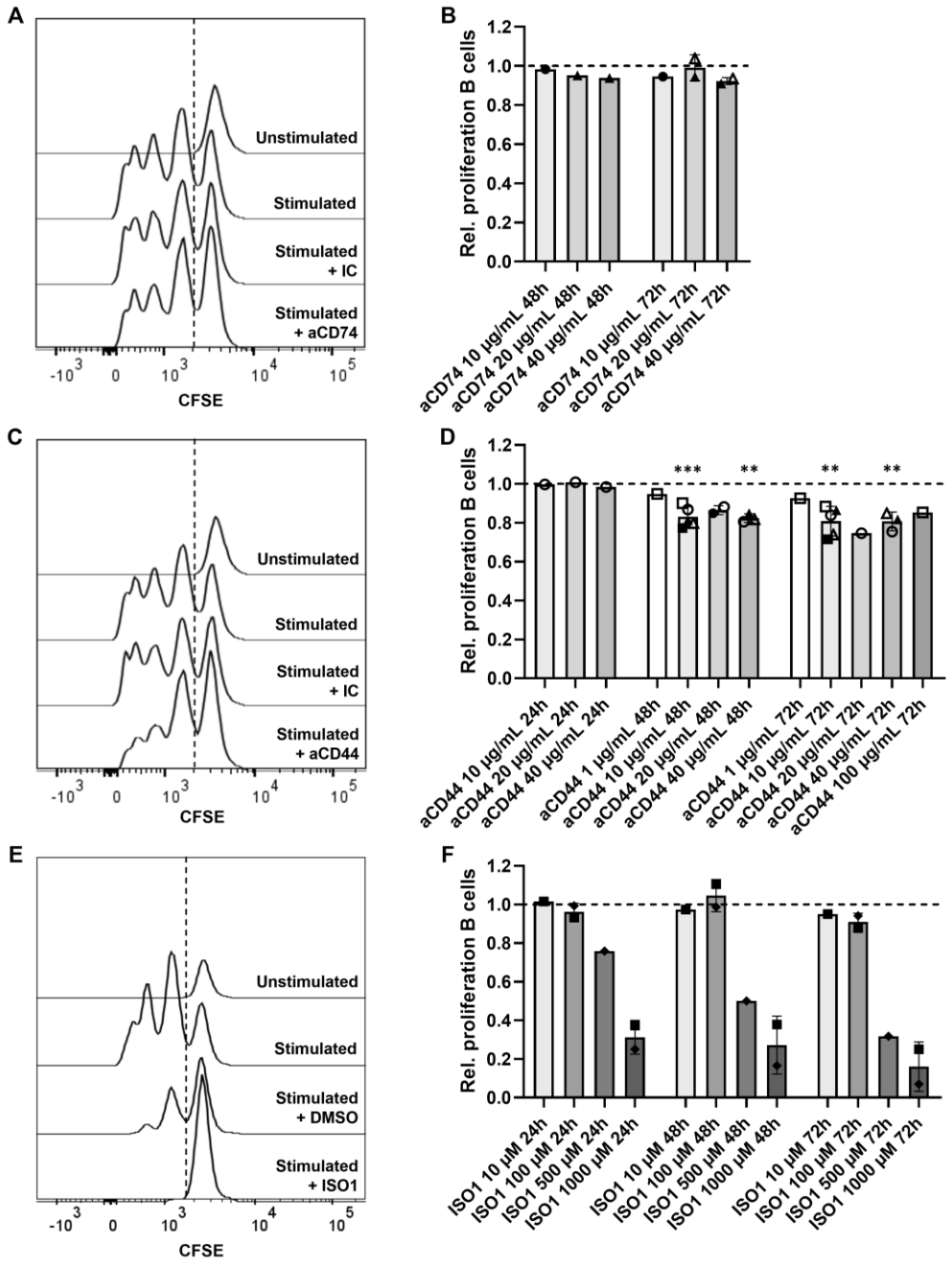

Figure 8 – Proliferation potential of B cells following CD74, CD44, and MIF blocking. B cells were isolated from the peripheral blood of HC (n=1-5) and *in vitro* activated with F(ab')$_2$ anti-human IgG/IgA/IgM, CpG2006 oligonucleotides, and CD40L. Following CD74 blocking (10, 20, and 40 µg/ml; **A-B**), CD44 blocking (1, 10, 20, 40, and 100 µg/ml; **C-D**), or MIF blocking (10, 100, 500, and 1000 µM; **E-F**) for 24, 48, or 72 hours, proliferation (% CFSE) was determined using flow cytometry. Proliferation histograms for CD74 and CD44 blocking (A and C) represent one measurement upon blocking with 40 µg/ml antibody or isotype control for 72 hours, whereas the histogram for MIF blocking (E) represents one measurement upon blocking with 1000 µM ISO1 or DMSO control for 72h. In the graphs (B, D, and F), each symbol represents the mean value of a different HC, measured in duplicates. Isotype controls were set at 1 (dotted line) and relative values were calculated based on the percentage (CFSE-based) of B cell proliferation. Data are shown as mean (bars) ± SD. Paired t-tests or Wilcoxon Signed-Rank tests were performed to compare proliferation upon receptor blocking to isotype controls. *$p < 0.05$, **$p < 0.01$, ***$p<0.001$. *aCD44, anti-CD44 blocking antibody; aCD74, anti-CD74 blocking antibody; CFSE,*

carboxyfluorescein succinimidyl ester; DMSO, dimethyl sulfoxide; h, hours; HC, healthy control; IC, isotype control; ISO1, (S,R)-3-(4-Hydroxyphenyl)-4,5-dihydro-5-isoxazole acetic acid; Rel., relative compared to isotype control.

Following incubation with MIF inhibitor (ISO1), only slight changes in CD80 expression were observed at concentrations of 10 to 500 µM (at 24h, 10 µM: 0,9144; 100 µM: 1.031 ± 0.001225; 500 µM: 1.054; at 48h, 10 µM: 1.016; 100 µM: 1.098 ± 0.01271; 500 µM: 0.9652; at 72h, 10 µM: 1.093; 100 µM: 1.045 ± 0.05054; 500 µM: 0.9549; Fig. 9E). The expression of the activation marker was mostly affected at the highest concentration (at 24h, 1000 µM: 0.6648 ± 0.1313; at 48h, 1000 µM: 0.8690 ± 0.03054; at 72h, 1000 µM: 0.8446 ± 0.2118; Fig. 9E). CD25 expression was not decreased upon MIF inhibition compared to treatment with DMSO for 24 hours (100 µM: 1.054; 500 µM: 1.167; 1000 µM: 1.068; Fig. 9F). Nevertheless, our results suggest a concentration-dependent reduction in CD25 expression at incubation times of 48 (10 µM: 1.123; 500 µM: 1.055; 1000 µM: 0.8443) and 72 hours (10 µM: 1,008; 500 µM: 0,9185; 1000 µM: 0.7998; Fig. 9F).

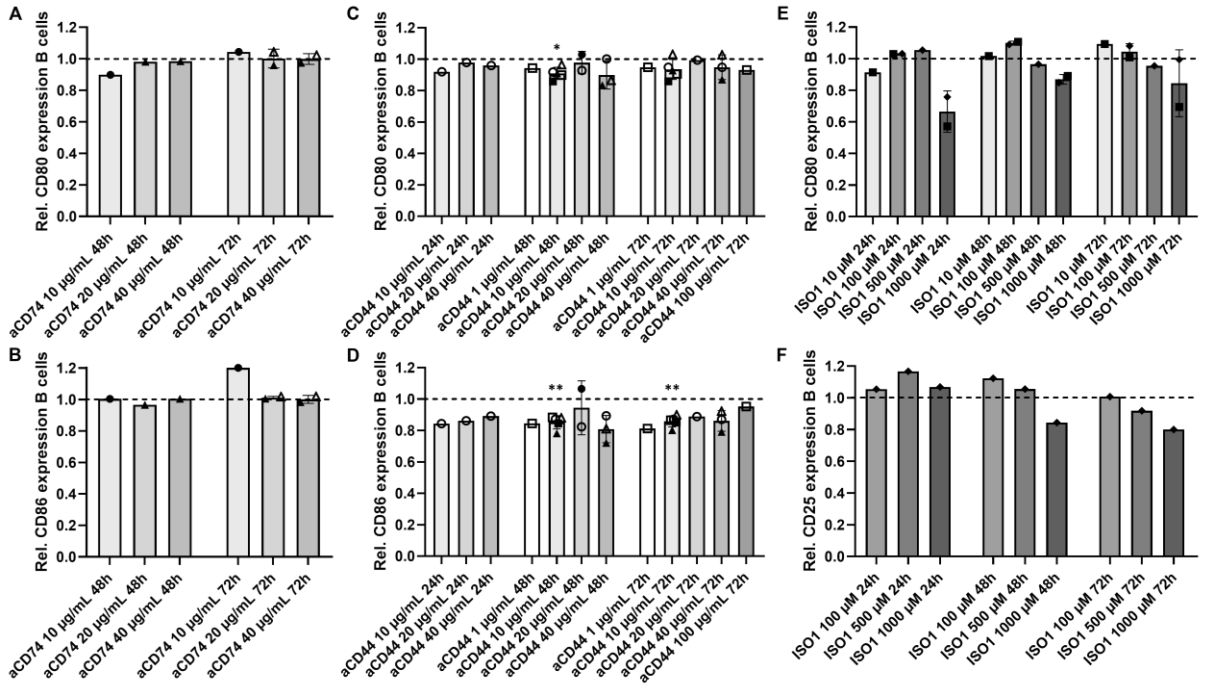

Figure 9 – Activation marker expression by B cells following CD74, CD44, and MIF blocking. B cells were isolated from the peripheral blood of HC (n=1-5) and *in vitro* activated with F(ab')$_2$ anti-human IgG/IgA/IgM, CpG2006 oligonucleotides, and CD40L. Following CD74 blocking (10, 20, and 40 µg/ml; **A-B**), CD44 blocking (1, 10, 20, 40, and 100 µg/ml; **C-D**), or MIF blocking (100, 500, and 1000 µM; **E-F**) for 24, 48, or 72 hours, the expression of activation markers (MFI of CD80, CD86, or CD25) was determined using flow cytometry. Each symbol represents the mean value of a different HC, measured in duplicates. Isotype controls were set at 1 (dotted line) and relative values were calculated based on the MFI of activation marker expression. Data are shown as mean (bars) ± SD. Paired t-tests or Wilcoxon Signed-Rank tests were performed to compare activation upon receptor blocking to isotype controls. *p < 0.05, **p < 0.01. *aCD44, anti-CD44 blocking antibody; aCD74, anti-CD74 blocking antibody; CD, cluster of differentiation; h, hours; IC, isotype control; ISO1, (S,R)-3-(4-Hydroxyphenyl)-4,5-dihydro-5-isoxazole acetic acid; MFI, median fluorescence intensity; Rel., relative compared to isotype control.*

DISCUSSION

In this study, the first steps towards understanding the role of the MIF/CD74 axis in post-SCI B cell responses were undertaken. We identified significant changes in absolute numbers of B cells and NK cells between different stages post-injury. In addition, a flow cytometry panel that

aims to study the MIF/CD74 axis in B cells and other immune cells in SCI patients was optimized. Further, in HC, we demonstrated a significant reduction in B cell proliferation and activation upon blocking the CD44 receptor and a markedly decreased trend in the proliferation of B cells upon MIF inhibition.

The study of general immune cell counts in whole blood at eight time points following injury indicated no significant differences for all studied subsets. Although statistical comparison to cell counts in the healthy situation was not possible due to the inclusion of only 2 HC, a trend towards increased mean levels of B cells, T cells, DC, and monocytes was observed at <1 week post-injury compared to HC. This could point to the early involvement and peripheral activation of these cells in SCI, potentially leading to their migration to the site of injury. Following the classification of time points in acute (≤4 weeks), subacute (7-18 weeks), and chronic (≥6 months) phases post-SCI, significant differences in B cells and NK cells were observed. Absolute B cell numbers were significantly higher in acute compared to subacute and chronic phases, suggesting their involvement in earlier stages of SCI and reflecting the peak of B cell infiltration observed in human spinal cord lesions at 4-21 days post-SCI (17). In contrast, for NK cells, significantly higher counts in the subacute and chronic compared to the acute phase, as well as a correlation with days post-injury were demonstrated. These findings may imply a role for NK cells beyond the acute phase of SCI.

Absolute numbers of B cells, T cells, DC, and monocytes have previously been studied in whole blood of SCI patients from <24 hours up to 136 days following injury (65). However, the use of a different time classification, the inclusion of individuals undergoing surgical intervention excluding the spinal cord as a control group instead of HC, and the expression of cell counts in a different unit, complicates the comparison with our results. In this previous report, rapid reductions in the studied cell subsets were demonstrated within 24 hours post-injury in patients compared to control subjects (65). Nevertheless, for all cell subsets, absolute numbers were significantly increased at one week compared to earlier stages (day 3-4), and T cells and DC remained elevated up to 30 days post-injury (65). In contrast, we did not observe significant differences in these or other immune cell subsets between <1 week and 3 or 4 weeks post-SCI. Moreover, in the same study, after one week, a decreasing trend in B cell numbers was observed with time, returning to levels of control subjects at 105-136 days post-SCI (65). Consistent with this trend, we observed significantly increased B cell numbers in acute versus subacute stages of SCI. Further, a case-control cohort study showed higher total leukocyte counts but lower lymphocyte counts in cervical SCI patients in comparison to control cases with spine trauma but normal neurologic evaluation within the first week post-injury (66). This conflicts with the increasing trend in B and T cells that was observed compared to HC in our study. However, it is crucial to consider the differences in cell counts between controls with spinal trauma and normal neurological evaluation and the HC in our study since we hypothesize that spine trauma with normal neurological evaluation is also associated with increased immune cell counts. Absolute NK cell numbers in whole blood have only been studied in a cohort of chronic SCI patients (3-217 months post-injury) in comparison to HC, where no significant differences but trends towards lower counts were observed (67).

Changes in immune cell subsets post-SCI have also been studied in PBMC instead of whole blood. In contrast to the variations in B cell counts observed here, we previously demonstrated no significant differences in total B cell frequencies in PBMC when comparing SCI patients ≤1 month post-injury, SCI patients >1 month post-injury, and HC (39). In the same study, we observed increased T cell frequencies in patients at >1 month compared to ≤1 month post-SCI, as well as in comparison to HC, consistent with a cross-sectional report that found elevated T cell frequencies in patients at varying time points >3 months post-SCI compared to HC (39, 68). No changes in T cell counts were shown here. Moreover, contrasting the increasing count of NK cells in whole blood with time post-injury, a longitudinal analysis of the frequency of NK cells in PBMC demonstrated significant decreases of NK cells at 0-3 days, 3, 6, and 12 months post-injury compared to HC. Nevertheless, we previously did not observe significant differences in NK cell frequencies in PBMC between SCI patients ≤1 month post-injury, SCI patients >1 month post-injury, and HC (39). However, when comparing immune cell frequencies in total PBMC and cell counts in whole

blood, it is important to consider that discrepancies between both may exist.

To confirm the increasing trends in B cell, T cell, DC, and monocyte counts at <1 week compared to HC reported in this study, the inclusion of more HC, allowing statistical analysis, is necessary. Moreover, a study with larger sample sizes and SCI patients and HC matched for age, biological sex, and sample size is needed, as the high variability among SCI patients, low variability among HC, and relatively low cell counts for HC in our cohort compared to previous studies could have influenced our results (69-71). To accurately interpret the observed differences in NK cells and B cells at stages post-injury, future studies should focus on comparing absolute cell counts and frequencies of these cell subsets at different stages post-injury, including HC in the analysis.

Previously, our research group demonstrated elevated frequencies of $CD74^+$ B cells in the peripheral blood of SCI patients in comparison to HC, suggesting the involvement of the MIF/CD74 axis in post-SCI B cell responses (39). Nevertheless, the expression of other components of the axis has not been studied in B cells and their subsets in the context of SCI before. Therefore, in this study, a spectral flow cytometry panel to study the expression of the MIF/CD74 axis in B cells and other immune cells was optimized. Our results showed that overnight intracellular MIF staining improved resolution beyond what was observed following 30 minutes of incubation, consistent with what has previously been reported for other intracellular proteins (72). Moreover, similar to previous reports, an improved signal was detected for staining of a chemokine receptor (CXCR2) at 37°C in NaN_3-free buffer (73-75). Similar resolutions at both 37°C and RT were observed for CD3, CD4, CD8, CD21, CD24, CD56, IgA, IgM, and HLA-DR, whereas CD11c, CD14, CD16, CD24, and CD45RA were preferably stained at RT. Lastly, negative and positive populations were well resolved upon simultaneous staining of Zombie NIR, IgG, CD11c, CD14, CD16, CD24, and CD45RA, minimizing staining steps and improving time efficiency. Following total evaluation, the panel can be used to study the MIF/CD74 axis in SCI patients versus HC.

Since the MIF/CD74 axis has previously been linked to pro-inflammatory B cell functions, we investigated the role of CD74, its co-receptor CD44, and MIF in primary B cell proliferation and activation upon general B cell stimulation. No significant differences in B cell proliferation and expression of activation markers CD80 and CD86, two co-receptors that stimulate T cells, were observed upon CD74 inhibition in all tested concentrations for 48 and 72 hours (76). This contrasts a study where substantial increases in proliferation, as measured by 5-bromo-2-deoxyuridine and [^{3}H] thymidine incorporation, were demonstrated upon stimulation of murine splenic B cells with an activating anti-CD74 antibody for 24 and 48 hours (44). This effect was CD74-specific since no differences in proliferation were detected following stimulation with isotype control or in splenic B cells from CD74 knockout mice (44). The same research group later demonstrated a reduction in the proliferation of splenic B cells isolated from CD74 knockout compared to control mice following MIF stimulation (48). Moreover, significantly reduced CFSE-based proliferation of primary human B cells has been observed upon anti-IgM stimulation and treatment with a CD74 blocking antibody compared to isotype control for 72 hours (43). In contrast to our results for CD74, we observed significant reductions in B cell proliferation and expression of CD80 and CD86 following inhibition of CD44, the co-receptor of CD74 in MIF signaling, for 48 and 72 hours. This is consistent with the reduced proliferation response that has been observed in splenic B cells from CD44 knockout in comparison to control mice (48).

Different hypotheses exist for the absence of an effect of CD74 blocking on B cell proliferation and activation. First of all, it is important to mention that statistical analysis could only be performed on measurements following the blocking of CD44, and more repeated measurements upon CD74 blocking should be performed to confirm our results. Moreover, differences in the antibody used to inhibit CD74 may influence results, as previous studies employed an anti-CD74 blocking antibody dissolved in a different buffer containing NaN_3, which has been demonstrated to affect in vitro PBMC proliferation (43, 77). This may have affected previous results since controlling for this effect was not mentioned (43). Alternatively, the differences in B cell proliferation and activation marker expression observed between CD44 and CD74 blocking might suggest that CD44 plays a

crucial role as the signaling component of the MIF/CD74 complex, whereas CD74 is primarily involved and needed for MIF binding. Future research should involve investigating the effects of simultaneous inhibition of both receptors on B cell proliferation and activation to confirm whether they synergistically reinforce pro-inflammatory B cell functions. Lastly, the possibility that the CD44 receptor is involved in B cell proliferation and activation via MIF/CD74 axis-independent pathways cannot be excluded. Therefore, the effect of CD44 blocking on these and other pro-inflammatory B cell functions should be further studied upon MIF stimulation only.

To study the role of MIF in B cell proliferation and activation, cells were treated with ISO1, a non-toxic cell-permeable antagonist of MIF that binds to its catalytically active site and inhibits the biological activities of MIF (78). Proliferation has only been studied following ISO1 administration upon simultaneous treatment with recombinant MIF in murine splenic B cells (48). A specific elevation in B cell proliferation, as measured by [^{3}H] thymidine incorporation, was demonstrated following MIF stimulation for 24 hours, which was abrogated in the presence of ISO1 (48). Here, we observed pronounced reductions in primary B cell proliferation upon MIF inhibition by treatment with ISO1 in the absence of MIF administration, with trends toward concentration- and duration-dependent effects. Although less pronounced than the effects on proliferation, trends have been observed in which high concentrations of ISO1 treatment result in reduced expression of the activation marker CD80. Additionally, high concentrations and long incubation times of ISO1 administration lead to trends of decreased CD25 expression, which is known to play a role in B cell antigen presentation (79). Although further research with larger sample sizes is needed, these results suggest that the presence of MIF is necessary for B cells to proliferate and may play a role in their ability to participate in T cell stimulation and antigen presentation. Therefore, it would be valuable to study the proliferation and expression of activation markers in B cells derived from SCI patients to confirm whether inhibiting CD44 and MIF results in similar or even more pronounced effects.

CONCLUSION

This study aimed to clarify the role of B cells and the MIF/CD74 axis in SCI pathology. Based on their absolute numbers present in the blood, our results suggest the involvement of B cells in earlier stages (≤4 weeks) and NK cells in later stages (≥7 weeks up to ≥6 months) post-injury. Future research should focus on studying the functional contribution of circulating B and NK cells to neuroinflammation and the peripheral immune response following SCI. Moreover, our findings in healthy individuals indicate that the co-receptor of CD74, CD44, as well as MIF, contribute to B cell activation and proliferation. Further studies in SCI patients are needed to confirm the significance of the MIF/CD74 axis in these and other pro-inflammatory functions of B cells post-injury.

REFERENCES

1. Ahuja CS, Wilson JR, Nori S, Kotter MRN, Druschel C, Curt A, et al. Traumatic spinal cord injury. Nat Rev Dis Primers. 2017;3:17018.
2. World Health Organization. Spinal Cord Injury. 2024 [Available from: https://www.who.int/news-room/fact-sheets/detail/spinal-cord-injury.
3. World Health Organization. Spinal cord injury: as many as 500 000 people suffer each year 2013 [Available from: https://www.who.int/news/item/02-12-2013-spinal-cord-injury-as-many-as-500-000-people-suffer-each-year.
4. Chen Y, He Y, DeVivo MJ. Changing Demographics and Injury Profile of New Traumatic Spinal Cord Injuries in the United States, 1972-2014. Arch Phys Med Rehabil. 2016;97(10):1610-9.
5. Lenehan B, Street J, Kwon BK, Noonan V, Zhang H, Fisher CG, et al. The epidemiology of traumatic spinal cord injury in British Columbia, Canada. Spine (Phila Pa 1976). 2012;37(4):321-9.
6. DeVivo MJ, Chen Y. Trends in new injuries, prevalent cases, and aging with spinal cord injury. Arch Phys Med Rehabil. 2011;92(3):332-8.
7. van den Berg ME, Castellote JM, Mahillo-Fernandez I, de Pedro-Cuesta J. Incidence of spinal cord injury worldwide: a systematic review. Neuroepidemiology. 2010;34(3):184-92; discussion 92.
8. Varma AK, Das A, Wallace Gt, Barry J, Vertegel AA, Ray SK, et al. Spinal cord injury: a review of current therapy, future treatments, and basic science frontiers. Neurochem Res. 2013;38(5):895-905.
9. Liu XZ, Xu XM, Hu R, Du C, Zhang SX, McDonald JW, et al. Neuronal and glial apoptosis after traumatic spinal cord injury. J Neurosci. 1997;17(14):5395-406.
10. Figley SA, Khosravi R, Legasto JM, Tseng YF, Fehlings MG. Characterization of vascular disruption and blood-spinal cord barrier permeability following traumatic spinal cord injury. J Neurotrauma. 2014;31(6):541-52.

11. Alizadeh A, Dyck SM, Karimi-Abdolrezaee S. Traumatic Spinal Cord Injury: An Overview of Pathophysiology, Models and Acute Injury Mechanisms. Front Neurol. 2019;10:282.
12. Griffiths IR, Miller R. Vascular permeability to protein and vasogenic oedema in experimental concussive injuries to the canine spinal cord. J Neurol Sci. 1974;22(3):291-304.
13. Tator CH, Koyanagi I. Vascular mechanisms in the pathophysiology of human spinal cord injury. J Neurosurg. 1997;86(3):483-92.
14. Norenberg MD, Smith J, Marcillo A. The pathology of human spinal cord injury: defining the problems. J Neurotrauma. 2004;21(4):429-40.
15. Fleming JC, Norenberg MD, Ramsay DA, Dekaban GA, Marcillo AE, Saenz AD, et al. The cellular inflammatory response in human spinal cords after injury. Brain. 2006;129(Pt 12):3249-69.
16. Xu GY, Hughes MG, Ye Z, Hulsebosch CE, McAdoo DJ. Concentrations of glutamate released following spinal cord injury kill oligodendrocytes in the spinal cord. Exp Neurol. 2004;187(2):329-36.
17. Zrzavy T, Schwaiger C, Wimmer I, Berger T, Bauer J, Butovsky O, et al. Acute and non-resolving inflammation associate with oxidative injury after human spinal cord injury. Brain. 2021;144(1):144-61.
18. Chang HT. Subacute human spinal cord contusion: few lymphocytes and many macrophages. Spinal Cord. 2007;45(2):174-82.
19. Jones TB, Basso DM, Sodhi A, Pan JZ, Hart RP, MacCallum RC, et al. Pathological CNS autoimmune disease triggered by traumatic spinal cord injury: implications for autoimmune vaccine therapy. J Neurosci. 2002;22(7):2690-700.
20. Popovich PG, Stokes BT, Whitacre CC. Concept of autoimmunity following spinal cord injury: possible roles for T lymphocytes in the traumatized central nervous system. J Neurosci Res. 1996;45(4):349-63.
21. Yoles E, Hauben E, Palgi O, Agranov E, Gothilf A, Cohen A, et al. Protective autoimmunity is a physiological response to CNS trauma. J Neurosci. 2001;21(11):3740-8.
22. Gris D, Marsh DR, Oatway MA, Chen Y, Hamilton EF, Dekaban GA, et al. Transient blockade of the CD11d/CD18 integrin reduces secondary damage after spinal cord injury, improving sensory, autonomic, and motor function. J Neurosci. 2004;24(16):4043-51.
23. Popovich PG, Guan Z, Wei P, Huitinga I, van Rooijen N, Stokes BT. Depletion of hematogenous macrophages promotes partial hindlimb recovery and neuroanatomical repair after experimental spinal cord injury. Exp Neurol. 1999;158(2):351-65.
24. Donnelly DJ, Longbrake EE, Shawler TM, Kigerl KA, Lai W, Tovar CA, et al. Deficient CX3CR1 signaling promotes recovery after mouse spinal cord injury by limiting the recruitment and activation of Ly6Clo/iNOS+ macrophages. J Neurosci. 2011;31(27):9910-22.
25. Ankeny DP, Guan Z, Popovich PG. B cells produce pathogenic antibodies and impair recovery after spinal cord injury in mice. J Clin Invest. 2009;119(10):2990-9.
26. Ankeny DP, Lucin KM, Sanders VM, McGaughy VM, Popovich PG. Spinal cord injury triggers systemic autoimmunity: evidence for chronic B lymphocyte activation and lupus-like autoantibody synthesis. J Neurochem. 2006;99(4):1073-87.
27. Casili G, Impellizzeri D, Cordaro M, Esposito E, Cuzzocrea S. B-Cell Depletion with CD20 Antibodies as New Approach in the Treatment of Inflammatory and Immunological Events Associated with Spinal Cord Injury. Neurotherapeutics. 2016;13(4):880-94.
28. Davies AL, Hayes KC, Dekaban GA. Clinical correlates of elevated serum concentrations of cytokines and autoantibodies in patients with spinal cord injury. Arch Phys Med Rehabil. 2007;88(11):1384-93.
29. Zajarias-Fainsod D, Carrillo-Ruiz J, Mestre H, Grijalva I, Madrazo I, Ibarra A. Autoreactivity against myelin basic protein in patients with chronic paraplegia. Eur Spine J. 2012;21(5):964-70.
30. Palmers I, Ydens E, Put E, Depreitere B, Bongers-Janssen H, Pickkers P, et al. Antibody profiling identifies novel antigenic targets in spinal cord injury patients. J Neuroinflammation. 2016;13(1):243.
31. Shen P, Fillatreau S. Antibody-independent functions of B cells: a focus on cytokines. Nat Rev Immunol. 2015;15(7):441-51.
32. Rastogi I, Jeon D, Moseman JE, Muralidhar A, Potluri HK, McNeel DG. Role of B cells as antigen presenting cells. Front Immunol. 2022;13:954936.
33. Pieper K, Grimbacher B, Eibel H. B-cell biology and development. J Allergy Clin Immunol. 2013;131(4):959-71.
34. De Silva NS, Klein U. Dynamics of B cells in germinal centres. Nat Rev Immunol. 2015;15(3):137-48.
35. Kurosaki T, Kometani K, Ise W. Memory B cells. Nat Rev Immunol. 2015;15(3):149-59.
36. Cunningham AF, Gaspal F, Serre K, Mohr E, Henderson IR, Scott-Tucker A, et al. Salmonella induces a switched antibody response without germinal centers that impedes the extracellular spread of infection. J Immunol. 2007;178(10):6200-7.
37. Bortnick A, Allman D. What is and what should always have been: long-lived plasma cells induced by T cell-independent antigens. J Immunol. 2013;190(12):5913-8.
38. Beckers L, Somers V, Fraussen J. IgD(-)CD27(-) double negative (DN) B cells: Origins and functions in health and disease. Immunol Lett. 2023;255:67-76.
39. Fraussen J, Beckers L, van Laake-Geelen CCM, Depreitere B, Deckers J, Cornips EMJ, et al. Altered Circulating Immune Cell Distribution in Traumatic Spinal Cord Injury Patients in Relation to Clinical Parameters. Front Immunol. 2022;13:873315.
40. Stumptner-Cuvelette P, Benaroch P. Multiple roles of the invariant chain in MHC class II function. Biochim Biophys Acta. 2002;1542(1-3):1-13.
41. Leng L, Metz CN, Fang Y, Xu J, Donnelly S, Baugh J, et al. MIF signal transduction initiated by binding to CD74. J Exp Med. 2003;197(11):1467-76.
42. Calandra T, Roger T. Macrophage migration inhibitory factor: a regulator of innate immunity. Nat Rev Immunol. 2003;3(10):791-800.
43. Rijvers L, Melief MJ, van der Vuurst de Vries RM, Stephant M, van Langelaar J, Wierenga-Wolf AF, et al. The macrophage migration inhibitory factor pathway in human B cells is tightly controlled and dysregulated in multiple sclerosis. Eur J Immunol. 2018;48(11):1861-71.

44. Starlets D, Gore Y, Binsky I, Haran M, Harpaz N, Shvidel L, et al. Cell-surface CD74 initiates a signaling cascade leading to cell proliferation and survival. Blood. 2006;107(12):4807-16.
45. Alampour-Rajabi S, El Bounkari O, Rot A, Muller-Newen G, Bachelerie F, Gawaz M, et al. MIF interacts with CXCR7 to promote receptor internalization, ERK1/2 and ZAP-70 signaling, and lymphocyte chemotaxis. FASEB J. 2015;29(11):4497-511.
46. Klasen C, Ohl K, Sternkopf M, Shachar I, Schmitz C, Heussen N, et al. MIF promotes B cell chemotaxis through the receptors CXCR4 and CD74 and ZAP-70 signaling. J Immunol. 2014;192(11):5273-84.
47. Bucala R, Shachar I. The integral role of CD74 in antigen presentation, MIF signal transduction, and B cell survival and homeostasis. Mini Rev Med Chem. 2014;14(14):1132-8.
48. Gore Y, Starlets D, Maharshak N, Becker-Herman S, Kaneyuki U, Leng L, et al. Macrophage migration inhibitory factor induces B cell survival by activation of a CD74-CD44 receptor complex. J Biol Chem. 2008;283(5):2784-92.
49. Shi X, Leng L, Wang T, Wang W, Du X, Li J, et al. CD44 is the signaling component of the macrophage migration inhibitory factor-CD74 receptor complex. Immunity. 2006;25(4):595-606.
50. Bernhagen J, Krohn R, Lue H, Gregory JL, Zernecke A, Koenen RR, et al. MIF is a noncognate ligand of CXC chemokine receptors in inflammatory and atherogenic cell recruitment. Nat Med. 2007;13(5):587-96.
51. Schwartz V, Lue H, Kraemer S, Korbiel J, Krohn R, Ohl K, et al. A functional heteromeric MIF receptor formed by CD74 and CXCR4. FEBS Lett. 2009;583(17):2749-57.
52. Lapter S, Ben-David H, Sharabi A, Zinger H, Telerman A, Gordin M, et al. A role for the B-cell CD74/macrophage migration inhibitory factor pathway in the immunomodulation of systemic lupus erythematosus by a therapeutic tolerogenic peptide. Immunology. 2011;132(1):87-95.
53. Thavayogarajah T, Sinitski D, El Bounkari O, Torres-Garcia L, Lewinsky H, Harjung A, et al. CXCR4 and CD74 together enhance cell survival in response to macrophage migration-inhibitory factor in chronic lymphocytic leukemia. Exp Hematol. 2022;115:30-43.
54. Su Y, Wang Y, Zhou Y, Zhu Z, Zhang Q, Zhang X, et al. Macrophage migration inhibitory factor activates inflammatory responses of astrocytes through interaction with CD74 receptor. Oncotarget. 2017;8(2):2719-30.
55. Koda M, Nishio Y, Hashimoto M, Kamada T, Koshizuka S, Yoshinaga K, et al. Up-regulation of macrophage migration-inhibitory factor expression after compression-induced spinal cord injury in rats. Acta Neuropathol. 2004;108(1):31-6.
56. Zhu Z, Hu Y, Zhou Y, Zhang Y, Yu L, Tao L, et al. Macrophage Migration Inhibitory Factor Promotes Chemotaxis of Astrocytes through Regulation of Cholesterol 25-Hydroxylase Following Rat Spinal Cord Injury. Neuroscience. 2019;408:349-60.
57. Zhang H, Hu YM, Wang YJ, Zhou Y, Zhu ZJ, Chen MH, et al. Macrophage migration inhibitory factor facilitates astrocytic production of the CCL2 chemokine following spinal cord injury. Neural Regen Res. 2023;18(8):1802-8.
58. Nishio Y, Koda M, Hashimoto M, Kamada T, Koshizuka S, Yoshinaga K, et al. Deletion of macrophage migration inhibitory factor attenuates neuronal death and promotes functional recovery after compression-induced spinal cord injury in mice. Acta Neuropathol. 2009;117(3):321-8.
59. Chalimoniuk M, King-Pospisil K, Metz CN, Toborek M. Macrophage migration inhibitory factor induces cell death and decreases neuronal nitric oxide expression in spinal cord neurons. Neuroscience. 2006;139(3):1117-28.
60. Zhou Y, Guo W, Zhu Z, Hu Y, Wang Y, Zhang X, et al. Macrophage migration inhibitory factor facilitates production of CCL5 in astrocytes following rat spinal cord injury. J Neuroinflammation. 2018;15(1):253.
61. Stein A, Panjwani A, Sison C, Rosen L, Chugh R, Metz C, et al. Pilot study: elevated circulating levels of the proinflammatory cytokine macrophage migration inhibitory factor in patients with chronic spinal cord injury. Arch Phys Med Rehabil. 2013;94(8):1498-507.
62. Bank M, Stein A, Sison C, Glazer A, Jassal N, McCarthy D, et al. Elevated circulating levels of the pro-inflammatory cytokine macrophage migration inhibitory factor in individuals with acute spinal cord injury. Arch Phys Med Rehabil. 2015;96(4):633-44.
63. Wu DM, Zheng ZH, Wang S, Wen X, Han XR, Wang YJ, et al. Association between plasma macrophage migration inhibitor factor and deep vein thrombosis in patients with spinal cord injuries. Aging (Albany NY). 2019;11(8):2447-56.
64. Asia, Committee ISIS. The 2019 revision of the International Standards for Neurological Classification of Spinal Cord Injury (ISNCSCI)-What's new? Spinal Cord. 2019;57(10):815-7.
65. Riegger T, Conrad S, Schluesener HJ, Kaps HP, Badke A, Baron C, et al. Immune depression syndrome following human spinal cord injury (SCI): a pilot study. Neuroscience. 2009;158(3):1194-9.
66. Furlan JC, Krassioukov AV, Fehlings MG. Hematologic abnormalities within the first week after acute isolated traumatic cervical spinal cord injury: a case-control cohort study. Spine (Phila Pa 1976). 2006;31(23):2674-83.
67. Campagnolo DI, Bartlett JA, Keller SE. Influence of neurological level on immune function following spinal cord injury: a review. J Spinal Cord Med. 2000;23(2):121-8.
68. Campagnolo DI, Dixon D, Schwartz J, Bartlett JA, Keller SE. Altered innate immunity following spinal cord injury. Spinal Cord. 2008;46(7):477-81.
69. Kokuina E, Breff-Fonseca MC, Villegas-Valverde CA, Mora-Diaz I. Normal Values of T, B and NK Lymphocyte Subpopulations in Peripheral Blood of Healthy Cuban Adults. MEDICC Rev. 2019;21(2-3):16-21.
70. Haller Hasskamp J, Zapas JL, Elias EG. Dendritic cell counts in the peripheral blood of healthy adults. Am J Hematol. 2005;78(4):314-5.
71. Bain BJ. Ethnic and sex differences in the total and differential white cell count and platelet count. J Clin Pathol. 1996;49(8):664-6.
72. Whyte CE, Tumes DJ, Liston A, Burton OT. Do more with Less: Improving High Parameter Cytometry Through Overnight Staining. Curr Protoc. 2022;2(11):e589.
73. Berhanu D, Mortari F, De Rosa SC, Roederer M. Optimized lymphocyte isolation methods for analysis of chemokine receptor expression. J Immunol Methods. 2003;279(1-2):199-207.

74. Anselmo A, Mazzon C, Borroni EM, Bonecchi R, Graham GJ, Locati M. Flow cytometry applications for the analysis of chemokine receptor expression and function. Cytometry A. 2014;85(4):292-301.
75. van Wolfswinkel M, van Meijgaarden KE, Ottenhoff THM, Niewold P, Joosten SA. Extensive flow cytometric immunophenotyping of human PBMC incorporating detection of chemokine receptors, cytokines and tetramers. Cytometry A. 2023;103(7):600-10.
76. Lenschow DJ, Sperling AI, Cooke MP, Freeman G, Rhee L, Decker DC, et al. Differential up-regulation of the B7-1 and B7-2 costimulatory molecules after Ig receptor engagement by antigen. J Immunol. 1994;153(5):1990-7.
77. Feldman SP, Mertelsmann R, Venuta S, Andreeff M, Welte K, Moore MA. Sodium azide enhancement of interleukin-2 production. Blood. 1983;61(4):815-8.
78. Al-Abed Y, Dabideen D, Aljabari B, Valster A, Messmer D, Ochani M, et al. ISO-1 binding to the tautomerase active site of MIF inhibits its pro-inflammatory activity and increases survival in severe sepsis. J Biol Chem. 2005;280(44):36541-4.
79. Brisslert M, Bokarewa M, Larsson P, Wing K, Collins LV, Tarkowski A. Phenotypic and functional characterization of human CD25+ B cells. Immunology. 2006;117(4):548-57.

Acknowledgements – First and foremost, HC is extremely grateful to JF and VS for offering her the opportunity to perform her senior internship in their research group and to be part of their interesting research. HC's gratitude extends to the University of Hasselt and the Biomedical Research Institute (BIOMED) for providing her an internship within their multidisciplinary institute. HC would like to express her deepest appreciation to SR, who guided and supported her during her senior internship. HC gained research skills and insights from her that will undoubtedly be invaluable for her future career. Moreover, HC would like to thank Ellen Sleurs and Laura Dusaer, who provided assistance in the lab. HC would also like to express gratitude to Lien Beckers, Elien Luyten, Astrid Pues, and everyone else of the research team. Further, HC wants to thank her fellow students and her parents, sister, and grandmother for their support.

Lastly, all authors would like to thank Kim Ulenaers, Igna Rutten (Hasselt University, Biomedical Research Institute and UBiLim), and the doctors and nurses of the involved hospitals and centres for sample collection and patient recruitment.

Author contributions – JF and SR conceived and designed the research project. SR supervised the research and HC carried out the experiments. SR acquired the samples on the flow cytometer. HC performed the data analysis, interpreted the results, designed the figures for this report, performed the statistical analysis, and wrote this paper with the support of SR. Ellen Sleurs and Laura Dusaer provided assistance with the experiments. All authors were involved in carefully editing the manuscript.

SUPPLEMENTARY INFORMATION

Supplementary Formula 1 – Formula to calculate absolute cell numbers.

$$Absolute\ Cell\ Count\ \left({}^{Cells}/_{\mu l}\right) = \frac{Cell\ Count}{Precision\ Count\ Beads\ Count}\ x\ Precision\ Count\ Beads\ Concentration\ ({}^{Beads}/_{\mu l})$$

Supplementary Table 1 – Detailed clinical information on SCI patients.

Subject	Age	Biological sex	AIS score		Location injury	Included time points
			At <1 week	Later time points		
SCI-01	41	F	B	B at 1y	Cervical	1y
SCI-02	75	M	D	D at 1y	Cervical	6m and 1y
SCI-03	59	M	N.A.	N.A.	Cervical	18w, 6m & 1y
SCI-04	62	M	N.A.	N.A.	Cervical	18w
SCI-05	60	M	N.A.	N.A.	Cervical	<1w & 3w
SCI-06	36	M	A	A at 2w	Cervical	<1w & 3w
SCI-07	24	M	A	A at 16w	Thoracic	<1w, 3w, 4w, 7w, 12w, 18w & 6m
SCI-08	48	M	N.A.	N.A.	Thoracic	3w, 4w, 7w, 12w, 18w & 6m
SCI-09	44	F	C	N.A.	Cervical	<1w & 3w
SCI-10	73	M	D	N.A.	Cervical	<1w, 7w, 12w & 18w
SCI-11	68	M	A	A at 6m	Thoracic	1y
SCI-12	73	M	D	D at 1y	Cervical	6m
SCI-13	75	M	D	D at 6m	Cervical	6m
SCI-14	33	F	D	D at 6m	Cervical	4w, 7w, 12w & 1y
SCI-15	35	M	C	C at 12w	Thoracic	7w, 12w & 6m
SCI-16	79	M	D	D at 6m	Cervical	12w & 6m

AIS, American Spinal Injury Association impairment scale; F, female; M, male; m, months post-injury; N.A., not available; SCI, spinal cord injury; w, weeks post-injury; y, year post-injury.

Supplementary Table 2 – Cell count panel used for flow cytometry.

Marker	Fluorochrome	Clone	Isotype	Supplier	Catalog number	Dilution
CD19	BV421	HIB-19	Mouse IgG1, κ	BioLegend	302233	1/50
CD3	FITC	HIT3a	Mouse IgG2a, κ	BioLegend	304027	1/100
CD56	PE-Dazzle594	HCD56	Mouse IgG1, κ	BioLegend	300306	1/50
CD14	BV605	M5E2	Mouse IgG2a, κ	BioLegend	318348	1/25
HLA-DR	AF700	I.243	Mouse IgG2a, κ	BioLegend	301834	1/50
CD45	PerCP-Cy5.5	HI30	Mouse IgG1, κ	BioLegend	307626	1/25

AF, Alexa Fluor; BV, Brilliant Violet; CD, cluster of differentiation; FITC, Fluorescein isothiocyanate; HLA-DR, Human Leukocyte Antigen DR isotype; Ig, immunoglobulin; PE, Phycoerythrin; PerCP-Cy, Peridinin chlorophyll protein-Cyanine.

Supplementary Table 3 – MIF/CD74 screening panel used for flow cytometry.

Marker	Fluorochrome	Clone	Isotype	Supplier	Catalog number	Dilution
CD3	Pacific Blue	UCHT1	Mouse IgG1, κ	BioLegend	300418	1/500

CD4	Spark Blue 574	SK3	Mouse IgG1, κ	BioLegend	344679	1/50
CD8	PerCP	SK1	Mouse IgG1, κ	BioLegend	344707	1/50
CD11c	BV711	3.9	Mouse IgG1, κ	BioLegend	301629	1/50
CD14	PE-Fire 700	S18004B	Mouse IgG1, κ	BioLegend	399221	1/2000
CD16	BV480	3G8	Mouse IgG1, κ	BD Biosciences	566171	1/200
CD19	APC-Fire 810	HIB19	Mouse IgG1, κ	BioLegend	302271	1/250
CD21	APC-Fire 750	Bu32	Mouse IgG1, κ	BioLegend	354919	1/20
CD24	BV605	ML5	Mouse IgG2a, κ	BioLegend	311123	1/20
CD27	BV510	M-T271	Mouse IgG1, κ	BioLegend	356420	1/20
CD38	BV421	HB-7	Mouse IgG1, κ	BioLegend	356617	1/100
CD44	FITC	IM7	Rat IgG2b, κ	BioLegend	103021	1/500
CD45RA	BV570	HI100	Mouse IgG2b, κ	BioLegend	304131	1/100
CD56 (NCAM)	PE-Fire 640	QA17A16	Mouse IgG1, κ (recombinant)	BioLegend	392431	1/200
CD74	PE	LN2	Mouse IgG1, κ	BioLegend	326807	1/20
CXCR2 (CD182)	PE-Cy7	5E8/CXCR2	Mouse IgG1, κ	BioLegend	320715	1/20
CXCR4 (CD184)	BV785	12G5	Mouse IgG2a, κ	BioLegend	306529	1/20
CXCR7	PE-Dazzle 594	8F11-M16	Mouse IgG2b, κ	BioLegend	331117	1/20
HLA-DR	PE-Fire 810	L243	Mouse IgG2a, κ	BioLegend	307683	1/100
IgA	PerCP-Vio 700	REA1014	Human IgG1 (recombinant)	Miltenyi Biotec	130-117-005	1/200
IgD	PE-Cy5	IA6-2	Mouse IgG2a, κ	BioLegend	348249	1/500
IgG	AF700	G18-145	Mouse IgG1, κ	BD Biosciences	561296	1/20
IgM	BV650	MHM-88	Mouse IgG1, κ	BioLegend	314525	1/100
MIF	AF647	932606	Mouse IgG1	R&D systems	IC2891R	1/80
Viability	Zombie NIR	/	/	BioLegend	423105	1/4000

APC, Allophycocyanin; AF, Alexa Fluor; BV, Brilliant Violet; CD, cluster of differentiation; CXCR, CXC-motif chemokine receptor; Cy, Cyanine; FITC, Fluorescein isothiocyanate; HLA-DR, Human Leukocyte Antigen DR isotype; Ig, immunoglobulin; MIF, macrophage migration inhibitory factor; NCAM, neural cell adhesion molecule; PE, Phycoerythrin; PerCP, Peridinin chlorophyll protein.

Supplementary Table 4 – Blocking antibodies and small molecule inhibitors with respective controls used for *in vitro* assays.

Specificity	Clone	Isotype	Supplier	Catalog number	Dilution
CD74	LN2	Mouse IgG1, κ	Southern Biotech	9775-14	10, 20, and 40 µg/ml
Isotype control	MG1-45		BioLegend	401407	
CD44	Hermes-1	Rat IgG2a, κ	ThermoFisher	MA4400	1, 10, 20, and 40 µg/ml
Isotype control	RTK2758		BioLegend	400543	
MIF (ISO1)	/	/	R&D Systems	4288/10	10, 100, 500, and 1000 µg/mL
DMSO			AppliChem	/	Same volume

CD, cluster of differentiation; DMSO, dimethyl sulfoxide; Ig, immunoglobulin; ISO1, (S,R)-3-(4-Hydroxyphenyl)-4,5-dihydro-5-isoxazole acetic acid; MIF, macrophage migration inhibitory factor.

Supplementary Table 5 – Activation assay antibody panel used for flow cytometry.

Marker	Fluorochrome	Clone	Isotype	Supplier	Catalog number	Dilution
CD19	BV650	HIB-19	Mouse IgG1, κ	BioLegend	302238	1/50
CD25*	BV785	BC96	Mouse IgG1, κ	BioLegend	302637	1/40
CD80	BV421	2D10	Mouse IgG1, κ	BioLegend	305222	1/20
CD86*	BV785	IT2.2	Mouse IgG2b, κ	BioLegend	305442	1/50
Viability	FVD-eFluor780	/	/	eBioscience	65-0865-14	1/1000

*Either CD25 or CD86 was included.

BV, Brilliant Violet; CD, cluster of differentiation; FVD, Fixable Viability Dye; Ig, immunoglobulin.

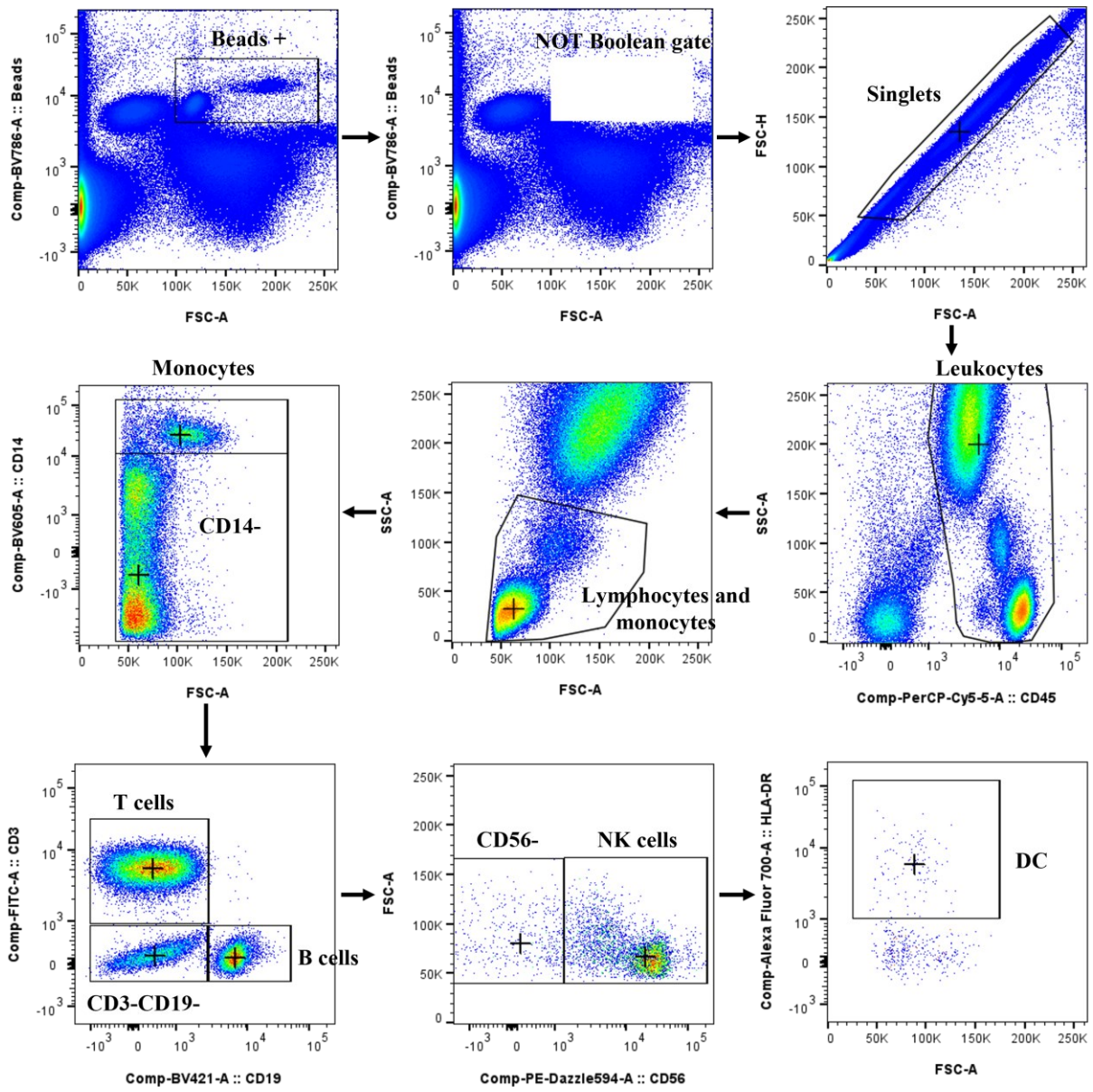

Supplementary Figure 1 – Representative gating strategy using count beads for determining the absolute number of major immune cell subsets in whole blood. The bead positive population was subtracted from the whole blood sample, after which the bead negative population was used for subsequent gating. The following markers were used to identify immune cell subsets ($CD45^+$): monocytes ($CD14^+$), B cells ($CD19^+$), T cells ($CD3^+$),

NK cells ($CD56^+$), and DC ($HLA\text{-}DR^+$). Dot plots of one representative SCI patient are shown. *DC, dendritic cells; FSC-A, forward scatter area; FSC-H, forward scatter height; HLA-DR, Human Leukocyte Antigen DR isotype; NK, natural killer; SSC-A, side scatter area.*

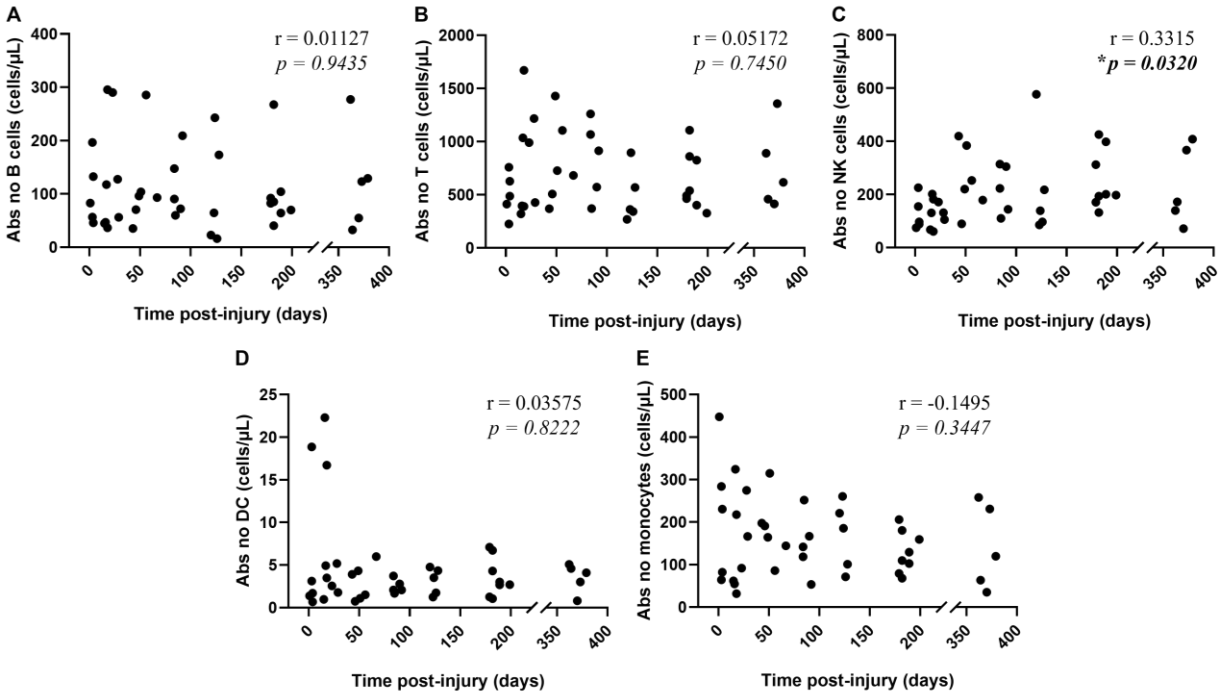

Supplementary Figure 2 – Correlation between the absolute number of major immune cell subsets and time post-injury. The absolute numbers (cells/µl) of B cells (**A**), T cells (**B**), NK cells (**C**), DC (**D**), and monocytes (**E**) in whole blood of SCI patients (n=16) were calculated using count beads at different time points post-injury. Spearman correlation tests were performed to study the correlation between the absolute number of major immune cell subsets (cells/µl) and time post-injury (days). The correlation coefficient and p-value are shown for each cell type. *$p < 0.05$. *DC, dendritic cells; NK, natural killer.*

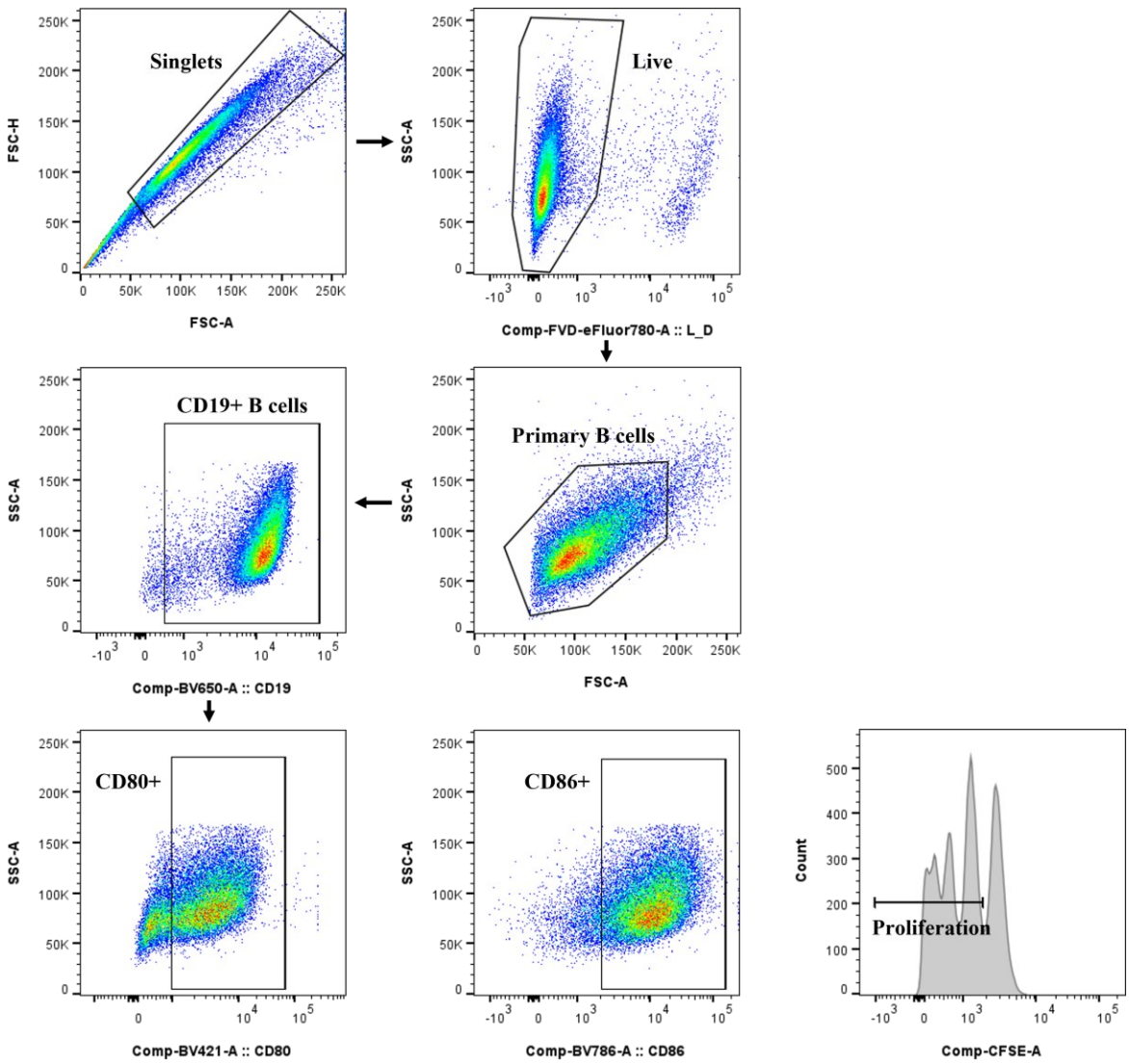

Supplementary Figure 3 – Representative gating strategy for studying *in vitro* proliferation and activation of B cells. B cells were identified based on the expression of surface marker CD19. Within this population, the expression of the activation markers CD80 and CD86 and CFSE-based proliferation was studied. The proliferation gate is set based on the unstimulated sample. Dot plots of one representative sample of B cells of a HC, activated with $F(ab')_2$ anti-human IgG/IgA/IgM, CpG2006 oligonucleotide, and CD40L, are shown. *CFSE, carboxyfluorescein succinimidyl ester; FSC-A, forward scatter area; FSC-H, forward scatter height; L_D, live-dead dye parameter; SSC-A, side scatter area.*